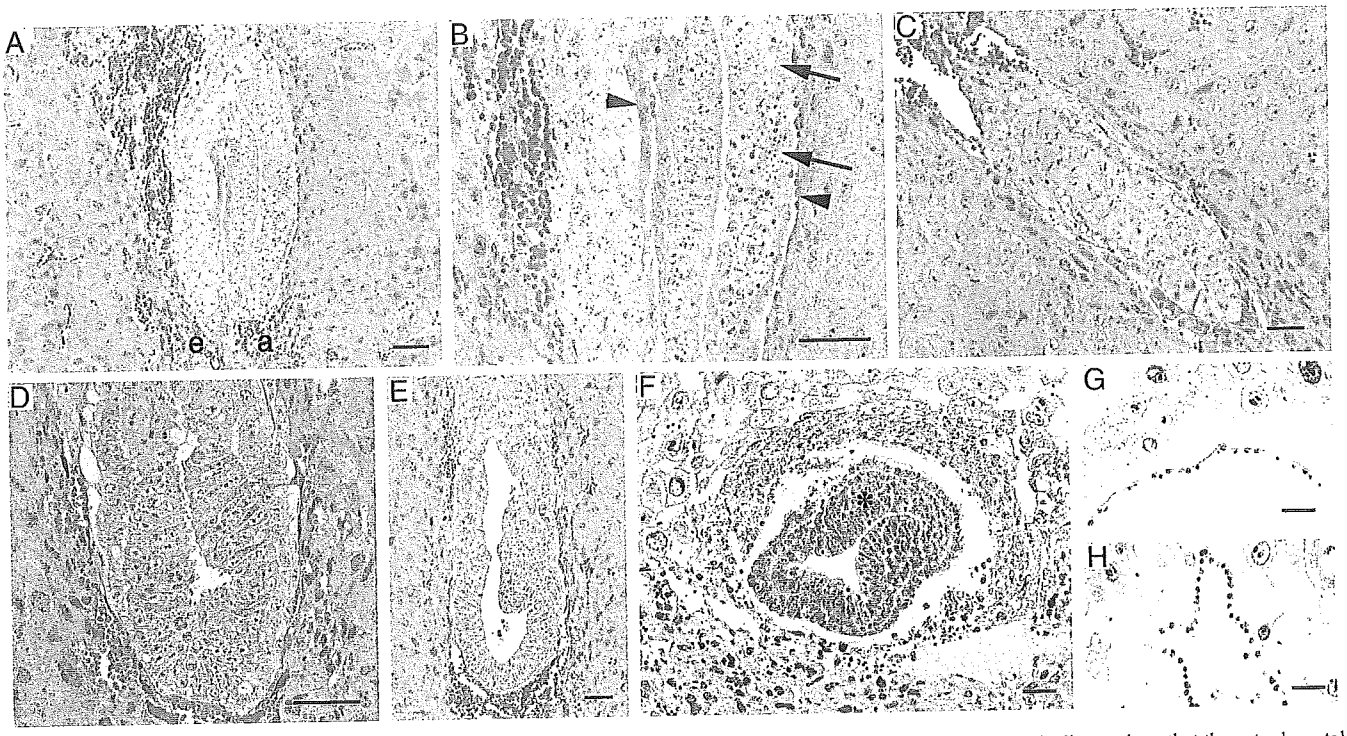

Fig. 1. Histological analysis of *fukutin*-null embryos. (A) Sagittal section of an E6.5 embryo. The axis of the egg cylinder is distorted, so that the ectoplacental cone (e) is attached to the apex (a). (B) Higher magnification of the same section. The concave face of the folded embryo lacks Reichert's membrane. Maternal red blood cells are present in the yolk sac cavity. The border between epiblast and visceral endoderm is obscure (arrows). Cells with pyknotic nuclei are clustered at the corresponding region. Red blood cells are observed in the yolk sac cavity (arrowheads). (C) Sagittal section of another E6.5 embryo. This embryo cannot be distinguished from wild type. (D) Sagittal section of an E7.5 embryo. The border between epiblast and visceral endoderm is obscure. Cells with pyknotic nuclei are occasionally observed. (E) Sagittal section of another E7.5 embryo. This embryo appears normal, with appropriate mesodermal differentiation. (F) Transverse section of an E8.5 embryo. Growth is severely retarded, although the embryo has initiated mesodermal differentiation (*). (G) Reichert's membrane of *fukutin*-null E8.5 embryo. (H) Reichert's membrane of wild-type E8.5 embryo. The bar in each panel corresponds to 100 μm.

two markers involved in patterning using whole mount in situ hybridization with *brachyury* and *Hesx1* probes in E7.5 and E8.5 embryos. Normally, *brachyury* is expressed in the primitive streak, the node, and the notochord (Kispert and Hermann, 1993). Homozygous-null embryos showed *brachyury* expression in the posterior domain, even in the misshaped specimens (Figs. 2A and B). The *Hesx1* probe detected proper expression in the anterior visceral endoderm at E7.5 and additional expression in the anterior neuroectoderm at E8.5 in both wild type and homozygous-null embryos (data not shown) (Thomas and Beddington, 1996).

An alternative possibility for the observed folding is that the abnormal Reichert's membrane limits embryo growth. To determine whether the parietal endoderm, which participates in producing Reichert's membrane, differentiates properly, we analyzed expression of *Gata-6* and *Pem*, markers specific for the parietal endoderm at E6.5. Since *Gata-6* probe yielded only a faint signal at this developmental stage, we could not judge the expression on parietal endoderm in both wild type and homozygous-null embryos, although it showed proper expression in the visceral endoderm (data not shown) (Morrisey et al., 1998). *Pem* is expressed in the visceral and parietal endoderm as well as in the extra embryonic ectoderm and ectoplacental cone in wild-type littermates (Lin et al., 1994). We observed a similar expression pattern for *Pem* in misshaped homozygous-null embryos (Figs. 2C and D). These observations suggest that the parietal endoderm undergoes proper differentiation in *fukutin*-null embryos.

Increased apoptotic cells in fukutin-null embryo

The increased number of cells with pyknotic nuclei indicates extensive apoptosis in the epiblast layer. To evaluate apoptosis levels more precisely, we performed a TUNEL assay on sections from E6.5, E7.5, and E8.5 embryos. We observed a significantly greater number of positive cells in homozygous-null embryos relative to wild-type control embryos. At E6.5 and E7.5, control embryos showed a small number of positive cells in the epiblast region, particularly around the cavity (Fig. 2E). In homozygous-null embryos, an increased number of apoptotic cells was distributed nonspecifically, predominantly in the epiblast region (Fig. 2F). Since all of the homozygous-null embryos at E8.5 showed growth retardation, direct comparison of apoptotic cell number in homozygous-null E8.5 embryos with that in age-matched control embryos may not be informative. Nevertheless, similar findings were obtained: in homozygous-null embryos, the number of TUNEL-positive cells was increased and confined to the epiblast region (Figs. 2G and H). By counting the number of positive cells in every other section of three wild type and three mutant embryos at E7.5, and then averaging the results, we found that the control embryos contained 3.3 ± 2.1 positive cells in epiblast per section, whereas the corresponding number for mutants was more than 3-fold higher (10.0 ± 3.5). We also counted positive cells per total cells in the epiblast region to circumvent the problem of growth retardation, demonstrating the increased apoptotic cells in *fukutin*-null embryo (5.6% for homozygous-null embryos versus 1.3% for wild type at E7.5, 14.2% versus 3.7% at E8.5).

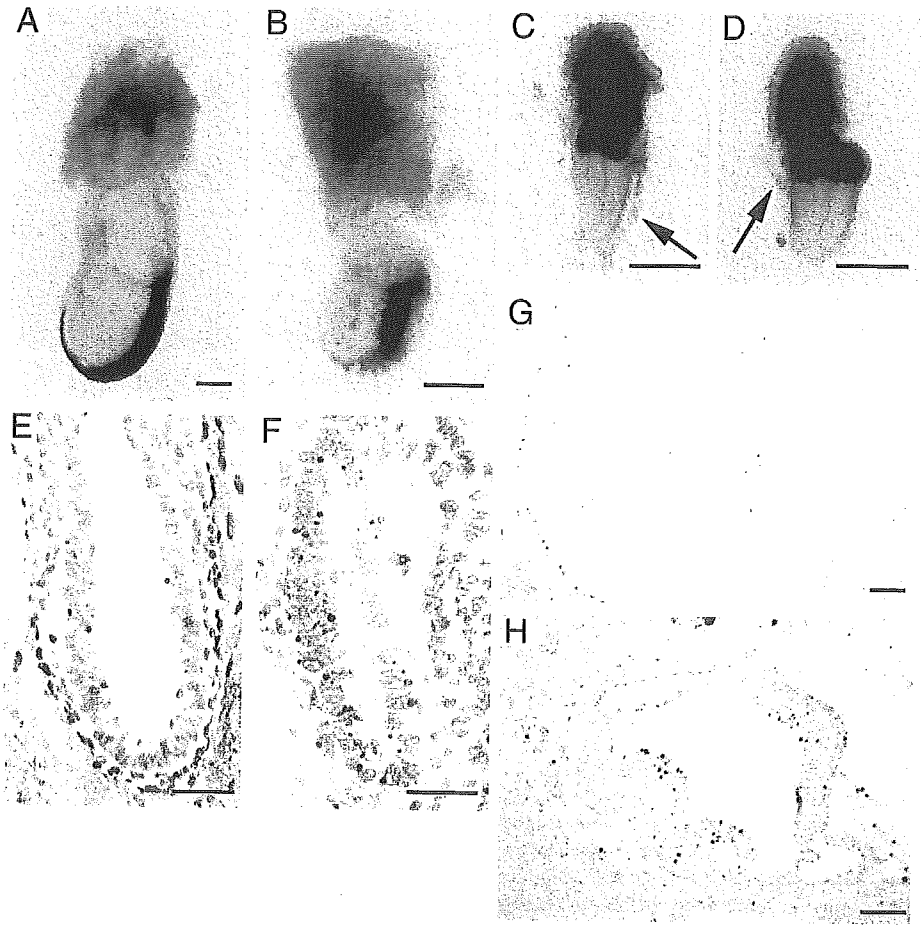

Fig. 2. Whole mount in situ hybridization and TUNEL analysis of *fukutin*-null embryos. (A and B) Whole mount in situ hybridization of *Brachyury* in E7.5 wild type (A) and homozygous-null (B) embryos. (C and D) Whole mount in situ hybridization of *Pem* in E6.5 wild type (C) and homozygous-null (D) embryos. Arrows indicate positive signals on Reichert's membranes. (E–H) TUNEL analysis of *fukutin*-null embryos. TUNEL was performed in sections from E7.5 wild type (E), E7.5 homozygous null (F), E8.5 wild type (G), and homozygous-null E8.5 embryos (H). The bar in each panel corresponds to 100 μm.

Hypoglycosylation of α-dystroglycan

Considerable evidence supports the view that fukutin function is associated with glycosylation of α-DG. To examine the glycosylation status of α-DG in wild type and *fukutin*-null embryos, we performed immunostaining with the anti α-DG antibody IIH6, which recognizes a sugar moiety associated with the laminin–α-DG interaction.

In wild-type E6.5 embryos, an anti-β-DG antibody yielded signals at the two BM regions (Fig. 3A) (Imamura et al., 2000). Glycosylation of α-DG, as evidenced by positive IIH6 staining, was also present in these BM regions as early as E6.5 in normal embryos (Fig. 3B).

Next, we compared the *fukutin*-null E8.5 embryos with wild-type control embryos. Control embryos showed positive signals at BM regions with both IIH6 and anti-β-DG antibodies. In *fukutin*-null embryos, the IIH6 signal was undetectable in this region in both severely and less severely affected embryos, despite the normal immunoreactivity of β-DG (Figs. 3C–H). The antibody VIA4 also recognizes sugar moieties in α-DG. We observed VIA4 immunoreactivity in E8.5 embryos, although at slightly reduced levels, suggesting that α-DG is still present but that the sugar moiety associated with laminin binding is reduced (Figs. 3I and J). In addition, heterozygous mutants showed IIH6 signals at BM regions comparable to the wild-type embryo (Fig. 3K).

If laminin binding by DG is disrupted in *fukutin*-null embryos, then it was reasonable to predict that laminin localization would also be abnormal. However, immunostaining with an anti-laminin antibody showed that localization patterns were preserved in mutant embryos (Figs. 4A and B). In addition, the reduced laminin-binding activity of α-DG may cause dysregulation of laminin subtypes. Since laminin α1 is a predominant laminin subtype at this developmental stage, we examined its subcellular localization by immunostaining with an anti-laminin α1 antibody. Like that of laminin, however, the laminin α1 staining pattern was also normal (Figs. 4E and F). Similarly, the immunoreactivity of collagen IV, another major BM component, was normal (Figs. 4C and D). Although our data indicate a reduction in the laminin-binding activity of α-DG in *fukutin*-null embryos, development of BM appears normal under light microscopic examination.

Basement membrane defect in fukutin-null mice

To analyze the structural differences in the BM between *fukutin*-null embryos and wild type, we performed electron microscopic examination on E6.5 embryos. First, we examined Reichert's membrane, which is composed of multiple distinct parallel layers between parietal endodermal cells and trophoblast cells, the outer parts of which resemble a common BM. In wild-type embryos, the thickness of Reichert's membrane was uniform,

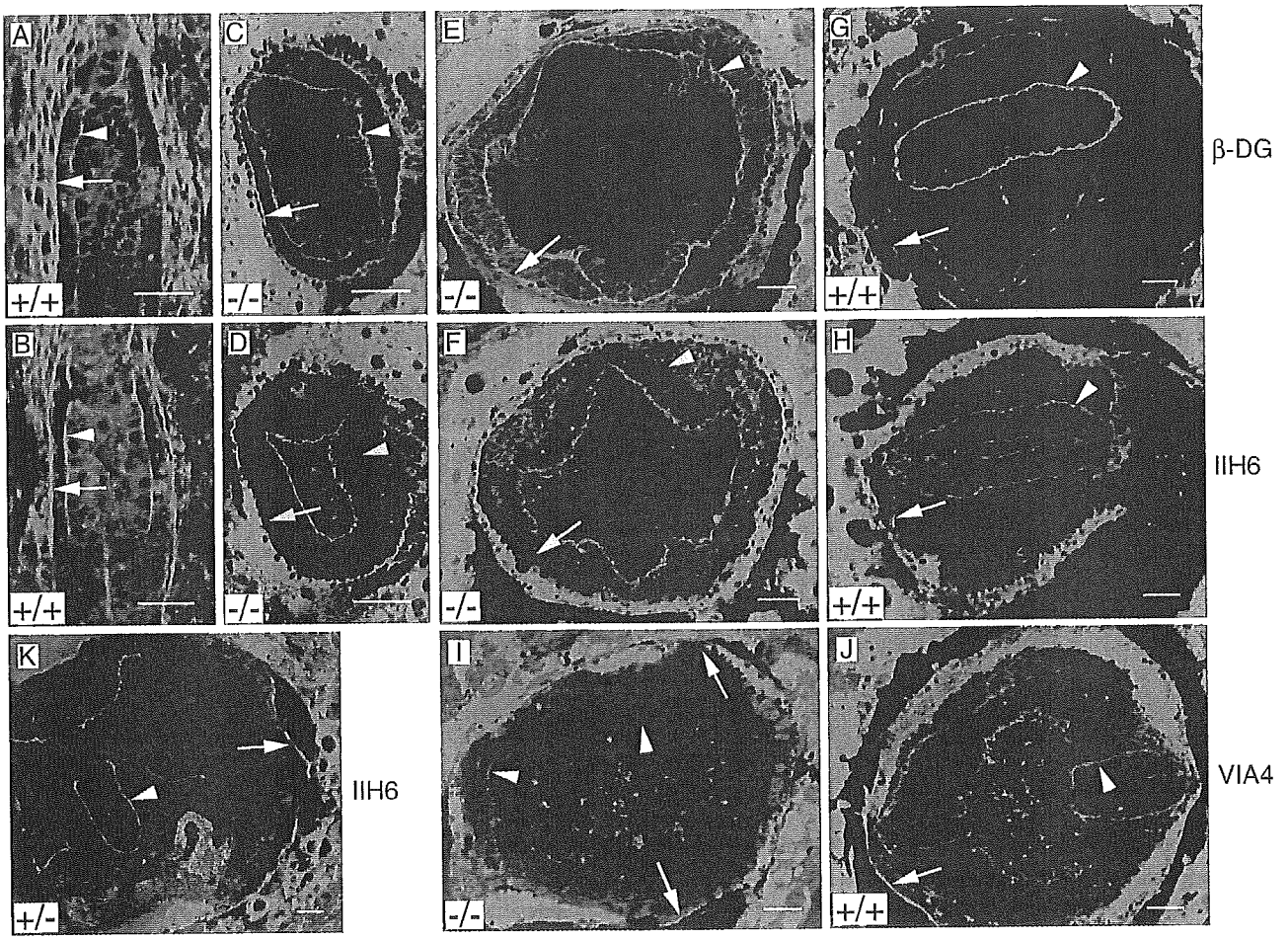

Fig. 3. Immunostaining on DG of *fukutin*-null embryos. (A–J) Immunostaining of *fukutin*-null embryos with anti-β-DG (A, C, E, and G), IIH6 (B, D, F, and H), which binds a sugar moiety at the laminin-binding site of α-DG, and VIA4 (I and J), which binds another sugar moiety of α-DG. At E6.5, DG is localized to two BM regions in wild-type embryos: Reichert's membrane (arrows) and the BM separating the epiblast and visceral endoderm (arrowheads) (A). α-DG glycosylation at the laminin binding site is already observed in the serial section of the same E6.5 wild-type embryo (B). At E8.5, the wild-type embryo also shows expression in the BM region (G, H, and J). In *fukutin*-null embryos, β-DG is expressed in a similar BM-specific pattern (C and E). The anti-α-DG antibody IIH6 does not show similar localization in the BM (D and F). Example BM regions lacking the IIH6 signal are indicated by yellow arrows and arrowheads. Staining surrounding the cavity at the center is nonspecific. However, the reduced but substantial VIA4 signal in BM regions in the serial section of the same embryo (I, arrows and arrowheads) suggests that α-DG is present, but glycosylation at laminin-binding sites does not occur in *fukutin*-null embryos. (K) Immunostaining of heterozygous mutant embryos with IIH6. Signals at BM region are comparable to those of wild-type embryo (arrow and arrowhead). The bar in each panel corresponds to 100 μm.

with a mean thickness of 687 ± 62 nm ($n = 4$) (Fig. 5A). Although this thickness varied among the *fukutin*-null embryos, the mean thickness (723 ± 319 nm, $n = 5$) resembled that of wild type. The membrane appeared wavy in homozygous-null embryos, however (Fig. 5B). For example, in one embryo, we observed variable thickness (ranging from 711 nm to 342 nm). Under higher magnification, the Reichert's membrane appeared fibrous in wild-type embryos, and a dense BM-like material was seen on the trophoblast-facing side (Fig. 5C). In *fukutin*-null embryos, this fibrous component appeared disorganized (Fig. 5D), and the membrane was often detached from the trophoblast. While this detachment was also seen in wild-type embryos, indicating a possible artifact, it was observed more often in *fukutin*-null embryos.

Next, we examined the BM between the ectodermal and endodermal cell layers. In wild type, the BM appeared to run parallel to the ectodermal cells' plasma membranes, covering the ectodermal cell layer (Fig. 5E). In contrast, the BM in homozygous-null embryos was entirely thin, partly detached from plasma membrane and partly breached (Fig. 5F). Apoptotic cells were occasionally seen, but we saw no correlation between the locations of the apoptotic cells and the breached BM. Duplication of the BM was observed frequently in wild-type embryos, indicating that the BM is actively replicated (Fig. 5E). However, we rarely observed this duplication in homozygous-null embryos.

Discussion

In this study, we have generated *fukutin*-null mice by targeted disruption of the *fukutin* gene. The embryonic lethality of these mice indicates that fukutin is functionally indispensable in early development. This is consistent with the previous observation that no human FCMD patients carrying point mutations on both alleles have been identified (Kondo-Iida et al., 1999). The retrotransposal mutation carried by most FCMD patients causes a reduction in

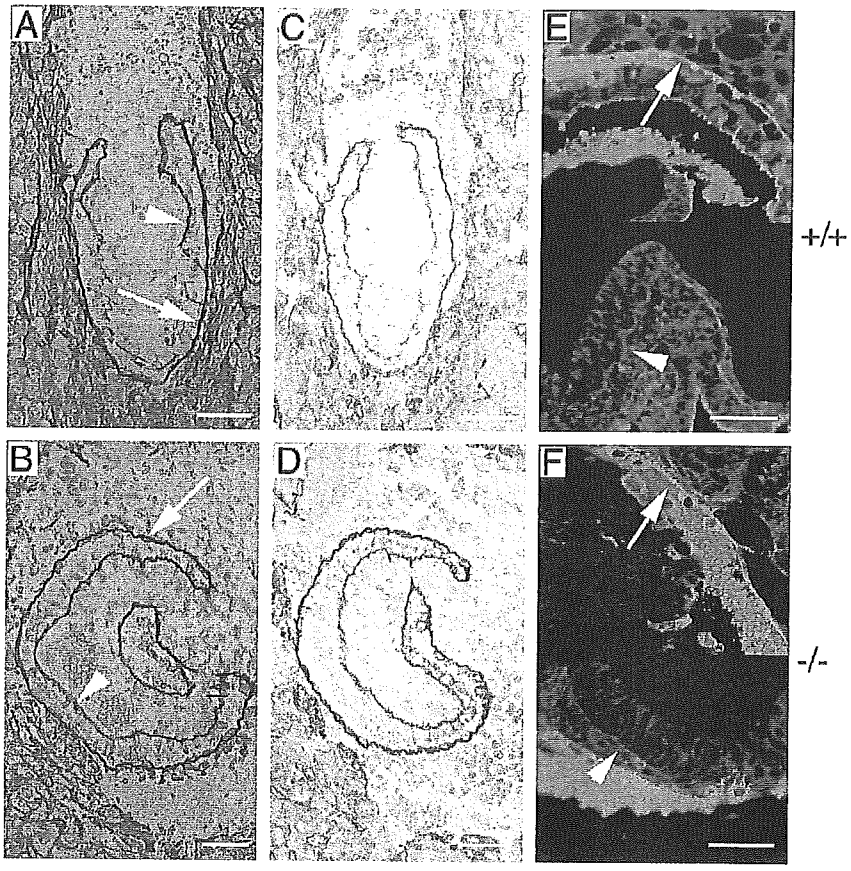

Fig. 4. Immunostaining on BM components of *fukutin*-null embryos. (A and B) Immunostaining with anti-laminin antibodies of E6.5 embryos. (C and D) Immunostaining with anti-collagen IV antibodies of E6.5 embryos. (E and F) Immunostaining with anti-laminin α1 antibodies of E8.5 embryos. These antibodies produced similar BM-specific localization patterns both in wild type (A, C, and E) and *fukutin*-null (B, D, and F) embryos. The bar in each panel corresponds to 100 μm.

fukutin transcript levels, but a small amount of fukutin protein is still produced from this allele. In FCMD patients who carry a point mutation and the retrotransposal mutation, enough fukutin protein is apparently produced to survive during this early embryonic stage. Recently, two patients with Walker–Warburg syndrome, which represents more severe phenotype than typical FCMD, were revealed to have a homozygous nonsense mutation in exon 4 or a homozygous 1-bp insertion in exon 5 of the *fukutin* gene (de Bernabe et al., 2003; Silan et al., 2003). Although these patients were born alive, both of them died on the 10th day or 4 months of age, much earlier than typical FCMD cases. Both of the mutations are likely to produce truncated fukutin protein, which might have some function and lead the embryo to escape the lethality.

Immunostaining of *fukutin*-null embryos demonstrates a reduced antigenicity against the sugar moiety of α-DG, indicating hypoglycosylation of α-DG. Since VIA4 signals were positive but faint in *fukutin*-null embryos, it is uncertain whether hypoglycosylated α-DG is still present on the membrane or not. It may also be possible that the membrane targeting of hypoglycosylated α-DG is impaired, or that hypoglycosylated α-DG is so unstable as to be degraded within a short period.

In any cases, hypoglycosylated α-DG lacks a laminin-binding site that is essential to the proper assembly of laminin, and deficiencies in this process presumably lead to BM defects. Targeted disruption of *DAG1* results in the loss of laminin assembly and discontinuity of the BM (Henry and Campbell, 1998; Williamson et al., 1997). *Fukutin*-null embryos share a number of phenotypes with *DAG1*-deficient mice. The distribution of *fukutin* expression is similar to that of *DAG1*, suggesting that fukutin also plays a pivotal role in BM development. Both *DAG1* and *fukutin*-null embryos show maternal red blood cells in the yolk sac cavity. However, in *fukutin*-null embryos, the BM is apparently normal under light microscopy, while physical alterations are apparent in *DAG1*-null embryos. Further, a recent finding in biological function of protein *O*-mannosyltransferase (POMT1), another glycosyltransferase that adds sugar moiety to α-DG and is responsible for Walker–Warburg syndrome, makes the issue more complicated. Targeted disruption of the gene causes serious BM abnormalities reminiscent of *DAG1*-null mice (Willer et al., 2004).

The expression and localization of the BM components laminin and collagen IV appear normal in *fukutin*-null embryos. Thus, while hypoglycosylation of α-DG reduces laminin-binding capacity, it does not abolish BM development completely. This suggests that residual sugar moieties also have laminin-binding capacity and sufficiently support the laminin assembly needed for proper BM development. On the other hand, laminin-binding capacity of α-DG might be completely abolished in *POMT1*-null embryo. Alternative conceivable explanation is that up-regulation of another laminin or collagen receptor may be able to compensate the function of α-DG in *fukutin*-null embryos.

It is reasonable to hypothesize that functional defects in the BM may be the primary cause of early lethality in *fukutin*-null embryos.

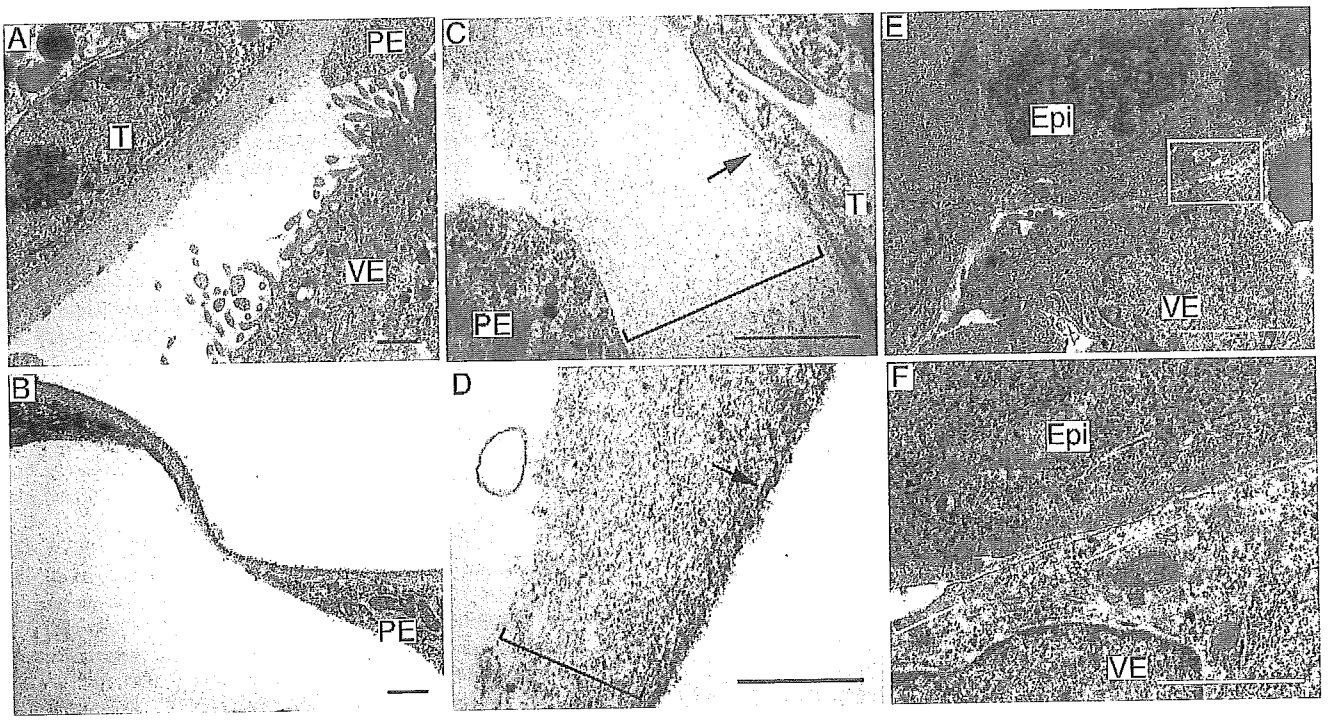

Fig. 5. Ultrastructural analysis of *fukutin*-null E6.5 embryos. (A) Reichert's membrane from a wild-type embryo. (B) Reichert's membrane from a *fukutin*-null embryo. The membrane appears wavy and partially thin. (C) Higher magnification of Reichert's membrane in wild-type embryo. Outer BM-like structures are indicated by arrows, while fibrous components are indicated by brackets. (D) Higher magnification of the *fukutin*-null embryo. (E) The BM separating ectoderm and visceral endoderm in a wild-type embryo. The BM appears as a continuous layer of membranous structure covering the ectoderm. Duplication of the BM is occasionally observed (box). (F) BM in a *fukutin*-null embryo. The BM is partially breached (brackets), and BM duplication is rarely observed. T, trophoblast; PE, parietal endoderm; VE, visceral endoderm; Epi, epiblast. The bar in each panel corresponds to 500 nm.

It is also possible that the subtle disorganization of BM that is undetectable under light microscopy causes a serious defect in *fukutin*-null embryos.

Electron microscopic analysis identified BM abnormalities in *fukutin*-null embryos that could not be detected by light microscopy. The BM and its related tissue, Reichert's membrane, appeared fragile and easily subject to breach. Ultrastructural BM abnormalities have been demonstrated previously in human FCMD tissue: thin and disrupted BM was observed in muscle (Ishii et al., 1997; Matsubara et al., 1999), and BM rupture was observed in brain (Nakano et al., 1996; Yamamoto et al., 1997a). A similar observation was reported in BM of FCMD fetus (Yamamoto et al., 1997b). Primary BM defects may cause the abnormal migration of neurons that leads to type 2 lissencephaly characteristic of FCMD. The disruption of BM and Reichert's membrane may also explain the leakage of maternal red blood cells into the yolk sac cavity. Therefore, BM fragility may be one of the primary etiologies for the phenotypes observed in *fukutin*-null embryos.

One of the most intriguing phenotypic abnormalities of *fukutin*-null embryos is the increased number of apoptotic cells present in the epiblast throughout early embryogenesis. In this early embryonic stage, two types of signals play pivotal roles in the generation of a cavity. The first, originating from endodermal cells, induces apoptosis of ectodermal cells to create the cavity. The second is a rescue signal, mediated by contact with the BM, which is required for the survival of the columnar epithelial cells that line the cavity (Coucouvanis and Martin, 1995). Targeted disruption of the genes encoding proteins that link the cellular membrane with the BM, such as laminin γ1, integrin β1, and *DAG1*, prevents BM generation, leading to embryonic lethality (Smyth et al., 1999; Stephens et al., 1995). Analysis of homozygous-null embryoid bodies has revealed an increase in apoptotic activity among ectodermal cells (Murray and Edgar, 2000). In *fukutin*-deficient mice, it is possible that the breached BM cannot transmit necessary survival signals to ectodermal cells via extracellular matrix/plasma membrane interactions, leading to the increased number of randomly distributed apoptotic cells. Dystroglycan, integrins, and other cell surface laminin receptors may play key roles in transducing such survival signals from the BM to cells (Li et al., 2003).

Another striking feature of the *fukutin*-null embryos is the folding and distortion of the embryo at the egg cylinder stage. Initially, we hypothesized that the abnormal expression of organizers that determine the embryonic axis may contribute to this phenotype. However, all of the relevant markers we examined showed normal expression patterns. While it is possible that the distribution of apoptotic cells may contribute to embryonic folding, we found no correlation between apoptotic cell localization and the direction of the folding. Ultrastructural examination showed that normal BM duplication is rarely observed in *fukutin*-null embryos, suggesting that the BM is not actively replicated. Since cells are proliferating rapidly in the developing embryo, the BM must be reconstituted at a rate proportional to the size of the embryo. Thus, it is possible that the observed size imbalance between the embryo and the BM in *fukutin*-null embryos may produce the observed folding. Integrin β1-deficient mice lack BM due to the down-regulation of laminin α1 expression (Aumailley et al., 2000). Reconstitution of the BM may require signaling through integrin β1, and *fukutin*-null embryos may have an impaired ability to transmit this signal.

All of the *fukutin*-null embryos examined showed growth retardation, ranging from severe to mild. This may result from an increase in apoptotic cells. Alternatively, BM dysfunction may result in a growth disadvantage caused by a deficiency in nutrients or soluble growth factors.

In our previous report, chimeric mice deficient in *fukutin* escaped the embryonic lethality and were born with FCMD phenotype (Takeda et al., 2003). One possible explanation is that extraembryonic tissues originating from blastocysts might be responsible for the lethality. In chimeric mice, homozygous-null cells might be rescued by presumably normal Reichert's membrane originating from wild-type extraembryonic cells. Alternatively, normal cells adjacent the homozygous-null cells might provide properly glycosylated α-DG through extracellular space and rescue the lethal BM dysfunction.

In summary, BM function is indispensable in early embryogenesis, and fukutin plays a pivotal role in BM function through glycosylation of α-DG. The phenotypic diversity seen in *fukutin*-null embryos may reflect multiple functional aspects of the BM, and these observed differences may be associated with the timing or location of BM disruption. Further analysis of *fukutin*-null mice will better elucidate multiple BM functions at various stages in embryonic development.

Acknowledgments

We thank Dr. Yukiko K. Hayashi and Dr. Eva Engvall for providing anti-laminin α1 antibody, Dr. Michihiro Imamura for anti-β-dystroglycan antibody, Dr. B. Hermann for the *Brachyury* plasmid, Dr. R. Beddington for the *Hesx1* plasmid, Dr. M.S. Parmacek for the *Gata6* plasmid, and Dr. C. L. MacLeod for the *Pem* plasmid. We also thank Takashi Wadatsu, Tomoyuki Iwanaga, Norihiro Miyazawa, and Mai Okano for mouse analysis; Eiji Oiki, Kyoko Mochida, and Yuko Nakabayashi for technical assistance; and Dr. Jennifer Logan for editing the manuscript. This work was supported by the 21st Century COE program from the Ministry of Education, Culture, Sports, Science, and Technology of Japan; and by a Health Science Research Grant, 'Research on Psychiatric and Neurological Diseases and Mental Health', and by a Research Grant for Nervous and Mental Disorders (14B-4), both from the Ministry of Health, Labor, and Welfare of Japan.

References

Aravind, L., Koonin, E.V., 1999. The fukutin protein family-predicted enzymes modifying cell-surface molecules. Curr. Biol. 9, R836–R837.

Aumailley, M., Pesch, M., Tunggal, L., Gaill, F., Fassler, R., 2000. Altered synthesis of laminin 1 and absence of basement membrane component deposition in β1 integrin-deficient embryoid bodies. J. Cell Sci. 113, 259–268.

Coucouvanis, E., Martin, G.R., 1995. Signals for death and survival: a two-step mechanism for cavitation in the vertebrate embryo. Cell 83, 279–287.

de Bernabe, D.B., van Bokhoven, H., van Beusekom, E., Van den Akker, W., Kant, S., Dobyns, W.B., Cormand, B., Currier, S., Hamel, B., Talim, B., Topaloglu, H., Brunner, H.G., 2003. A homozygous nonsense mutation in the fukutin gene causes a Walker–Warburg syndrome phenotype. J. Med. Genet. 40, 845–848.

Grewal, P.K., Holzfeind, P.J., Bittner, R.E., Hewitt, J.E., 2001. Mutant glycosyltransferase and altered glycosylation of α-dystroglycan in the myodystrophy mouse. Nat. Genet. 28, 151–154.

Hayashi, Y.K., Ogawa, M., Tagawa, K., Noguchi, S., Ishihara, T., Nonaka, I., Arahata, K., 2001. Selective deficiency of α-dystroglycan in Fukuyama-type congenital muscular dystrophy. Neurology 57, 115–121.

Henry, M.D., Campbell, K.P., 1998. A role for dystroglycan in basement membrane assembly. Cell 95, 859–870.

Horie, M., Kobayashi, K., Takeda, S., Nakamura, Y., Lyons, G.E., Toda, T., 2002. Isolation and characterization of the mouse ortholog of the Fukuyama-type congenital muscular dystrophy gene. Genomics 80, 482–486.

Imamura, M., Araishi, K., Noguchi, S., Ozawa, E., 2000. A sarcoglycan-dystroglycan complex anchors Dp116 and utrophin in the peripheral nervous system. Hum. Mol. Genet. 9, 3091–3100.

Ishii, H., Hayashi, Y.K., Nonaka, I., Arahata, K., 1997. Electron microscopic examination of basal lamina in Fukuyama congenital muscular dystrophy. Neuromuscular Disord. 7, 191–197.

Kano, H., Kobayashi, K., Herrmann, R., Tachikawa, M., Manya, H., Nishino, I., Nonaka, I., Straub, V., Talim, B., Voit, T., Topaloglu, H., Toda, T., Endo, T., 2002. Deficiency of α-dystroglycan in muscle-eye-brain disease. Biochem. Biophys. Res. Commun. 291, 1283–1286.

Kispert, A., Hermann, B.G., 1993. The Brachyury gene encodes a novel DNA binding protein. EMBO J. 12, 4898–4899.

Kobayashi, K., Nakahori, Y., Miyake, M., Matsumura, K., Kondo-Iida, E., Nomura, Y., Segawa, M., Yoshioka, M., Saito, K., Osawa, M., Hamano, K., Sakakihara, Y., Nonaka, I., Nakagome, Y., Kanazawa, I., Nakamura, Y., Tokunaga, K., Toda, T., 1998. An ancient retrotransposal insertion causes Fukuyama-type congenital muscular dystrophy. Nature 394, 388–392.

Kondo-Iida, E., Kobayashi, K., Watanabe, M., Sasaki, J., Kumagai, T., Koide, H., Saito, K., Osawa, M., Nakamura, Y., Toda, T., 1999. Novel mutations and genotype–phenotype relationships in 107 families with Fukuyama-type congenital muscular dystrophy (FCMD). Hum. Mol. Genet. 8, 2303–2309.

Li, S., Edgar, D., Fassler, R., Wadsworth, W., Yurchenco, P.D., 2003. The role of laminin in embryonic cell polarization and tissue organization. Dev. Cell 4, 613–624.

Lin, T.P., Labosky, P.A., Grabel, L.B., Kozak, C.A., Pitman, J.L., Kleeman, J., MacLeod, C.L., 1994. Pem homeobox gene is X-linked and exclusively expressed in extraembryonic tissues during early murine development. Dev. Biol. 166, 170–179.

Matsubara, S., Mizuno, Y., Kitaguchi, T., Isozaki, E., Miyamoto, K., Hirai, S., 1999. Fukuyama-type congenital muscular dystrophy: close relation between changes in the muscle basal lamina and plasma membrane. Neuromuscular Disord. 9, 388–398.

Michele, D.E., Campbell, K.P., 2003. Dystrophin–glycoprotein complex: post-translational processing and dystroglycan function. J. Biol. Chem. 278, 15457–15460.

Michele, D.E., Barresi, R., Kanagawa, M., Saito, F., Cohn, R.D., Satz, J.S., Dollar, J., Nishino, I., Kelley, R.I., Somer, H., Straub, V., Mathews, K.D., Moore, S.A., Campbell, K.P., 2002. Post-translational disruption of dystroglycan–ligand interactions in congenital muscular dystrophies. Nature 418, 417–422.

Morrisey, E.E., Tang, Z., Sigrist, K., Lu, M.M., Jiang, F., Ip, H.S., Parmacek, M.S., 1998. GATA6 regulates HNF4 and is required for differentiation of visceral endoderm in the mouse embryo. Genes Dev. 12, 3579–3590.

Murray, P., Edgar, D., 2000. Regulation of programmed cell death by basement membranes in embryonic development. J. Cell Biol. 150, 1215–1221.

Nakano, I., Funahashi, M., Takada, K., Toda, T., 1996. Are breaches in the glia limitans the primary cause of the micropolygyria in Fukuyama-type congenital muscular dystrophy (FCMD)? Pathological study of the cerebral cortex of an FCMD fetus. Acta Neuropathol. (Berl.) 91, 313–321.

Silan, F., Yoshioka, M., Kobayashi, K., Simsek, E., Tunc, M., Alper, M., Cam, M., Guven, A., Fukuda, Y., Kinoshita, M., Kocabay, K., Toda, T., 2003. A new mutation of the fukutin gene in a non-Japanese patient. Ann. Neurol. 53, 392–396.

Smyth, N., Vatansever, H.S., Murray, P., Meyer, M., Frie, C., Paulsson, M., Edgar, D., 1999. Absence of basement membranes after targeting the LAMC1 gene results in embryonic lethality due to failure of endoderm differentiation. J. Cell Biol. 144, 151–160.

Stephens, L.E., Sutherland, A.E., Klimanskaya, I.V., Andrieux, A., Meneses, J., Pedersen, R.A., Damsky, C.H., 1995. Deletion of β1 integrins in mice results in inner cell mass failure and peri-implantation lethality. Genes Dev. 9, 1883–1895.

Takeda, S., Kondo, M., Sasaki, J., Kurahashi, H., Kano, H., Arai, K., Misaki, K., Fukui, T., Kobayashi, K., Tachikawa, M., Imamura, M., Nakamura, Y., Shimizu, T., Murakami, T., Sunada, Y., Fujikado, T., Matsumura, K., Terashima, T., Toda, T., 2003. Fukutin is required for maintenance of muscle integrity, cortical histiogenesis and normal eye development. Hum. Mol. Genet. 12, 1449–1459.

Thomas, P., Beddington, R., 1996. Anterior primitive endoderm may be responsible for patterning the anterior neural plate in the mouse embryo. Curr. Biol. 6, 1487–1496.

Toda, T., Segawa, M., Nomura, Y., Nonaka, I., Masuda, K., Ishihara, T., Sakai, M., Tomita, I., Origuchi, Y., Ohno, K., Misugi, N., Sasaki, Y., Takada, K., Kawai, M., Otani, K., Murakami, T., Saito, K., Fukuyama, Y., Shimizu, T., Kanazawa, I., Nakamura, Y., 1993. Localization of a gene for Fukuyama type congenital muscular dystrophy to chromosome 9q31–33. Nat. Genet. 5, 283–286.

Toda, T., Kobayashi, K., Takeda, S., Sasaki, J., Kurahashi, H., Kano, H., Tachikawa, M., Wang, F., Nagai, Y., Taniguchi, K., Taniguchi, M., Sunada, Y., Terashima, T., Endo, T., Matsumura, K., 2003a. Fukuyama-type congenital muscular dystrophy (FCMD) and alpha-dystroglycanopathy. Congenit. Anom. 43, 97–104.

Toda, T., Kobayashi, K., Takeda, S., Sasaki, J., Kurahashi, H., Kano, H., Tachikawa, M., Wang, F., Nagai, Y., Taniguchi, K., Taniguchi, M., Sunada, Y., Terashima, T., Endo, T., Matsumura, K., 2003b. Fukuyama-type congenital muscular dystrophy and abnormal glycosylation of α-dystroglycan. Basic Appl. Myol. 13, 287–292.

Willer, T., Prados, B., Falcon-Perez, J.M., Renner-Muller, I., Przemeck, G.K., Lommel, M., Coloma, A., Valero, M.C., de Angelis, M.H., Tanner, W., Wolf, E., Strahl, S., Cruces, J., 2004. Targeted disruption of the Walker–Warburg syndrome gene Pomt1 in mouse results in embryonic lethality. Proc. Natl. Acad. Sci. U. S. A. 101, 14126–14131.

Williamson, R.A., Henry, M.D., Daniels, K.J., Hrstka, R.F., Lee, J.C., Sunada, Y., Ibraghimov-Beskrovnaya, O., Campbell, K.P., 1997. Dystroglycan is essential for early embryonic development: disruption of Reichert's membrane in Dag1-null mice. Hum. Mol. Genet. 6, 831–841.

Yamamoto, T., Shibata, N., Kanazawa, M., Kobayashi, M., Komori, T., Kondo, E., Saito, K., Osawa, M., 1997a. Early ultrastructural changes in the central nervous system in Fukuyama congenital muscular dystrophy. Ultrastruct. Pathol. 21, 355–360.

Yamamoto, T., Toyoda, C., Kobayashi, M., Kondo, E., Saito, K., Osawa, M., 1997b. Pial–glial barrier abnormalities in fetuses with Fukuyama congenital muscular dystrophy. Brain Dev. 19, 35–42.

Yoshida, A., Kobayashi, K., Manya, H., Taniguchi, K., Kano, H., Mizuno, M., Inazu, T., Mitsuhashi, H., Takahashi, S., Takeuchi, M., Herrmann, R., Straub, V., Talim, B., Voit, T., Topaloglu, H., Toda, T., Endo, T., 2001. Muscular dystrophy and neuronal migration disorder caused by mutations in a glycosyltransferase, POMGnT1. Dev. Cell 1, 717–724.

PERGAMON

Neuromuscular Disorders 15 (2005) 416–426

www.elsevier.com/locate/nmd

Effects of fukutin deficiency in the developing mouse brain

Tomohiro Chiyonobu[a,1], Junko Sasaki[a,1], Yoshitaka Nagai[a], Satoshi Takeda[b], Hiroshi Funakoshi[c], Toshikazu Nakamura[c], Tohru Sugimoto[d], Tatsushi Toda[a,*]

[a]*Division of Functional Genomics, Department of Post-Genomics and Diseases, Osaka University Graduate School of Medicine, 2-2-B9 Yamadaoka, Suita, Osaka 565-0871, Japan*
[b]*Otsuka GEN Research Institute, Otsuka Pharmaceutical Co. Ltd, 463-10 Kagasuno, Kawauchi-cho, Tokushima 771-0192, Japan*
[c]*Division of Molecular Regenerative Medicine, Osaka University Graduate School of Medicine, B-7, Osaka 565-0871, Japan*
[d]*Department of Pediatrics, Graduate School of Medical Science, Kyoto Prefectural University of Medicine, 465 Kajii-cho, Kamigyo-ku, Kyoto 602-8566, Japan*

Received 14 October 2004; received in revised form 2 February 2005; accepted 16 March 2005

Abstract

The major pathological change in Fukuyama-type congenital muscular dystrophy brain is polymicrogyria. Pathological studies of Fukuyama-type congenital muscular dystrophy brain indicated that protrusion of neurons into the subarachnoid space through breaches in the glia limitans–basal lamina complex is a cardinal pathogenic process in this condition. It remains undetermined, however, whether the defect causing this abnormal migration resides in the migrating neurons or in the glia limitans–basal lamina complex. To elucidate the pathogenesis of brain abnormalities in Fukuyama-type congenital muscular dystrophy, we analyzed histologically and immunohistochemically the developing forebrain in fukutin-deficient chimeric mice and compared it with that in controls ($n=4$ in each group). In chimeric embryos, ectopia became apparent as early as embryonic day 14, and laminar organization became progressively distorted. The basal lamina of the cortical surface in chimeras showed defects at E14, coinciding with the earliest time point at which ectopia were detected. Immunohistochemical analysis of glycosylated α-dystroglycan showed progressive defects coincidental with the disruption of the basal lamina. Neuronal migration was not affected in chimeras, as determined by detection of bromodeoxyuridine-labeled neurons. Extension of radial glial fibers was intact in chimeras. Taken together, disruption of the basal lamina, caused by the loss of interaction between hypoglycosylated α-dystroglycan and its ligands, plays a key role in the pathogenesis of cortical dysplasia in Fukuyama-type congenital muscular dystrophy.

Keywords: Fukuyama-type congenital muscular dystrophy; Fukutin; α-Dystroglycan; Glycosylation; Basal lamina; Neuronal migration

1. Introduction

Fukuyama-type congenital muscular dystrophy (FCMD; MIM 253800), one of the most common autosomal recessive disorders in Japan, is characterized by severe congenital muscular dystrophy associated with brain malformation and ocular abnormalities [1]. These clinical manifestations are similar to those seen in muscle–eye–brain disease (MEB; MIM 253280) and Walker–Warburg syndrome (WWS; MIM 236670) [2,3], implying that similar pathogenic mechanisms underlie all these diseases. Through positional cloning, we previously identified the gene responsible for FCMD, named *fukutin*, on chromosome 9q31. The predominant FCMD-causing mutation, also thought to be the ancestral founder mutation, is a 3 kb retrotransposal insertion in the 3′ untranslated region of the *fukutin* gene. This mutation reduces *fukutin* mRNA levels and is thought to cause the FCMD phenotype due to loss of function of *fukutin*. Disease-causing point mutations in *fukutin* also have been identified [4].

Although the function of fukutin protein remains unconfirmed, several lines of evidence suggest a functional linkage between fukutin and proper glycosylation of α-dystroglycan (α-DG). First, fukutin is a Golgi-resident protein, and it shares some homology with fringe-like

* Corresponding author. Tel.: +81 6 6879 3380; fax: +81 6 6879 3389.
E-mail address: toda@clgene.med.osaka-u.ac.jp (T. Toda).
[1] These authors contributed equally to this work.

0960-8966/$ - see front matter © 2005 Elsevier B.V. All rights reserved.
doi:10.1016/j.nmd.2005.03.009

glycosyltransferases [4,5]. Second, immunoreactivity against the sugar moiety of α-DG is selectively deficient in skeletal muscle from FCMD patients [6]. Finally, it was recently demonstrated that hypoglycosylated α-DG core protein, which cannot bind key ligands, is expressed at the muscle surface of FCMD patients [7].

The major pathological change in FCMD brain is polymicrogyria, although a various degree of cortical dysplasia is found in each case [1]. The pathogenic mechanisms underlying the brain abnormalities caused by fukutin deficiency remain undetermined, however. Pathological studies of brain tissue from FCMD fetuses and adults have revealed extrusion of neuroglial tissue into the subarachnoid space through breaches in the glia limitans (GL)–basal lamina (BL) complex [8–10], but it is unclear whether disruption of the GL–BL complex is the cause or consequence of aberrant neuronal migration. Several reports suggest that fukutin may play a role in neuronal migration because of its predominant expression in neurons [11,12]. On the other hand, fukutin expression has been observed in glial cells, including astrocytes, suggesting that fukutin is important in the integrity of GL [13].

Homozygous germline disruption of the *fukutin* gene in mice results in early embryonic lethality, limiting studies of fukutin function during mouse embryonic development [14]. Recently, we successfully generated fukutin-deficient chimeric mice, which recapitulate the major phenotypes of FCMD, using embryonic stem (ES) cells targeted for both *fukutin* alleles [15]. Chimeric mice with a high contribution of fukutin-deficient cells develop abnormalities in neuronal migration that mimic those of FCMD patients, in addition to severe muscular dystrophy and ocular abnormalities. Thus, these mice are suitable models for studying the pathogenesis of FCMD. In the present study, we performed histological and immunohistochemical analyses on the developing forebrain in fukutin-deficient chimeric mice at various embryonic stages to elucidate the underlying pathogenic mechanisms of brain abnormalities in FCMD.

2. Materials and methods

2.1. Experimental animals

The present series of experiments were conducted using fukutin-deficient chimeric mice. We investigated the developing forebrain of chimeric embryos showing 80% or greater contribution of fukutin-deficient cells ($n=4$ at each embryonic days). These mice develop laminar disorganization of cortical structures in the brain, which are associated with muscular dystrophy [15]. Littermate embryos with a fewer than 10% contribution of fukutin-deficient cells do not develop obvious phenotypes and were used as controls ($n=4$ at each embryonic days). The contribution rate of fukutin-deficient cells was determined using DNA extracted from the tail of each embryo (see below), because the extent of chimerism in various tissues is nearly equivalent [15]. Experimental protocols strictly followed the Ethical Committee Guidelines for Animal Experimentation of Osaka University.

2.2. Evaluation of the contribution rate of fukutin-deficient ES cells in chimeric mice

Genomic DNA was isolated from the tail of each chimeric mouse embryo using a standard technique. PCR was performed to amplify specific sequences in the wild-type allele (exon 2 of the *fukutin* gene) and the targeted allele (the neomycin resistance gene) [15]. The primers designed for the wild-type allele were F: 5′-ACGTGTACTGCCATACTTGG-3′ and R: 5′-TAGTGCTTGTAGTAGTACAGC-3′ (295 bp). The primers designed for the targeted allele were F: 5′-GGATCGATTCTAGGAATTCTC-3′ and R: 5′-ACTTCCTGACTAGGGGAGG-3′ (240 bp). PCR conditions for the wild-type allele were as follows: 2 min denaturation at 94 °C, followed by 25 amplification cycles (30 s, 94 °C; 30 s, 58 °C; 30 s, 72 °C), and a final 5 min extension at 72 °C. PCR conditions for the targeted allele were as follows: 2 min denaturation at 94 °C, followed by 28 amplification cycles (30 s, 94 °C; 30 s, 58 °C; 30 s, 72 °C), and a final 5 min extension at 72 °C. Equal volumes of both PCR products were mixed and separated electrophoretically on 3% agarose gels and visualized by staining with ethidium bromide. The contribution rate of fukutin-deficient cells was estimated by comparing the relative intensities of the two bands with PCR products amplified from control genomic template mixtures containing known ratios (0:10, 2:8, 4:6, 6:4, 8:2, and 10:0) of genomic DNA derived from targeted and wild-type ES cells.

2.3. Histology and immunohistochemistry

Embryos were removed from pregnant mice, fixed in ascending ethanol series at 4 °C, embedded in paraffin, and sectioned to 8 μm thickness at sagittal. Sections were stained with hematoxylin and eosin or immunostained with a polyclonal antibody against Engelbreth–Holm–Swarm (EHS) laminin (Harbor Bio-products), a monoclonal anti-α-DG antibody (clone IIH6C4, Upstate Biotechnology), or a monoclonal anti-nestin antibody (clone Rat 401, BD Biosciences). For immunohistochemistry, deparaffinized sections were blocked with 5% goat serum in MOM Mouse Ig Blocking Reagent (Vector Laboratories) for 1 h at room temperature and incubated with primary antibodies diluted in MOM Diluent (Vector Laboratories) overnight at 4 °C. After incubation with Alexa Fluor 488 or 546-labeled secondary antibodies (Molecular Probes) for 1 h at room temperature, sections were examined under a fluorescent microscope.

2.4. Western blotting

Whole brain tissue from E18 embryos was homogenized in ten-fold volume of homogenization buffer (PBS containing 1% Triton X-100 and protease inhibitors). After incubation for 30 min at 4 °C, protein extracts were centrifuged for 10 min at 4 °C and 15,000 × *g*. The resulting supernatants were rotated overnight at 4 °C with 100 μl of wheat germ agglutinin (WGA)–Sepharose 6 MB (Amersham Pharmacia). The affinity beads were then washed and boiled for 5 min in sample buffer containing 50 mM Tris HCl (pH 6.8), 2% SDS, glycerol, and 2-mercaptoethanol.

Extracted samples were separated electrophoretically on 7.5 (for α-DG) and 10% (for β-dystroglycan (β-DG)) SDS-polyacrylamide gels and transferred to polyvinylidene difluoride membrane (Millipore). Blots were probed using anti-β-DG antibody (clone 8D5, Novocastra Laboratories), anti-α-DG antibody (clone IIH6C4) and anti-core α-DG antibody (kindly provided by Kevin Campbell, Howard Hughes Medical Institute, University of Iowa) [7]. Signals were detected with peroxidase-conjugated secondary antibodies, using SuperSignal West Pico (Pierce) as a chemiluminescent substrate.

2.5. In vivo migration assay

For bromodeoxyuridine (BrdU) labeling, pregnant mice bearing E13 embryos were injected intraperitoneally with BrdU (100 μg/g body weight, dissolved in PBS). Embryos were removed from pregnant mice at E14 and E18, fixed in 4% paraformaldehyde/PBS overnight at 4 °C, embedded in paraffin, and cut into 8 μm sagittal sections. After deparaffinizing, sections were quenched for 30 min with 0.3% H_2O_2/methanol, treated with 2 N HCl for 1 h to denature DNA, neutralized for 5 min with 0.1 M sodium borate buffer (pH 8.5), blocked for 20 min with 10% horse serum/PBS, and incubated with a monoclonal anti-BrdU antibody (Takara) overnight at 4 °C. Sections were then washed in PBS and incubated for 30 min with peroxidase-conjugated rabbit anti-mouse IgG antibody (DAKO). The color was developed with 3,3′-diaminobenzidine tetrahydrochloride, and the slides were counterstained with hematoxylin.

The quantitative distribution of BrdU-labeled cells in the cortices was determined from photomicrographs covering the entire cortical depth, which were subdivided into three equidistant horizontal bands from pial to ventricular surface. The number of BrdU-labeled cells was counted in each horizontal band of the cortices and was expressed as a percentage of all labeled cells in the entire thickness of the cortices. These percentages were used in the statistical analysis (i.e. Student *t*-test). Cells that had nuclei with a mottled or punctuate reaction product were not counted as labeled, since these cells were considered to have just entered or left the S-phase while BrdU was available.

3. Results

3.1. Histological findings of the developing forebrain

To investigate the effects of fukutin deficiency on the developing forebrain and to determine when brain abnormalities first appear, we prepared histological sections from E12, E14, and E18 embryos. At E12, no differences were apparent between chimeras and controls (Fig. 1A and B). By E14, the cerebral cortices of chimeras had become wavy in appearance, and developing ectopia could be observed (Fig. 1C). The developing ectopia could be seen as small groups of neurons invading into the subarachnoid space (Fig. 1C). At E18, the cortices of chimeras were covered by a mantle of abnormal neuroglial tissue, and the laminar organization in the cortices became progressively more distorted (Fig. 1E). In contrast, cortices in control E18 embryos showed well-organized lamination (Fig. 1F).

3.2. Basal lamina of the cortical surface

To determine whether the BL of the cortical surface is perturbed in fukutin-deficient chimeras, we performed immunohistochemical analyses of laminin distribution in the developing forebrain. In control embryos at all developmental stages, the BL covered the pial surface of the cortices continuously, evidenced by consistent laminin immunoreactivity (Fig. 2B, D, and F). In chimeras, the BL appeared intact only at an early stage (E12) of cortical development (Fig. 2A). By E14, when ectopia coincidentally appeared, laminin immunreactivity in the BL had become discontinuous (Fig. 2C). At E18, laminin immunoreactivity in chimeras had disappeared almost completely from the BL of cortical surface but remained intact around blood vessels (Fig. 2E).

To investigate the correlation between α-DG and the BL, we next analyzed glycosylated α-DG distribution in the developing forebrain. The anti-α-DG antibody used in immunohistochemistry (IIH6C4) recognizes the laminin-binding sugar moiety of α-DG but does not recognize the core protein [7]. Whereas glycosylated α-DG was continuously present on the cortical surface in control embryos at all ages (Fig. 3B, D, and F), it became progressively defective with age in chimeras (Fig. 3A, C, and E). Overall, the immunoreactivity of glycosylated α-DG paralleled that of laminin in both chimeras and controls at all ages. Western blotting of WGA-enriched homogenates from E18 brain of chimeras demonstrated a significant glycosylation defect of α-DG. In brain from chimeras, glycosylated α-DG reactive to IIH6C4 is absent, but core α-DG antibody showed that α-DG is expressed and reduced in molecular mass (Fig. 4). These observations indicate a strong correlation between glycosylation of α-DG and maintenance of BL integrity in the developing forebrain of fukutin-deficient chimeras.

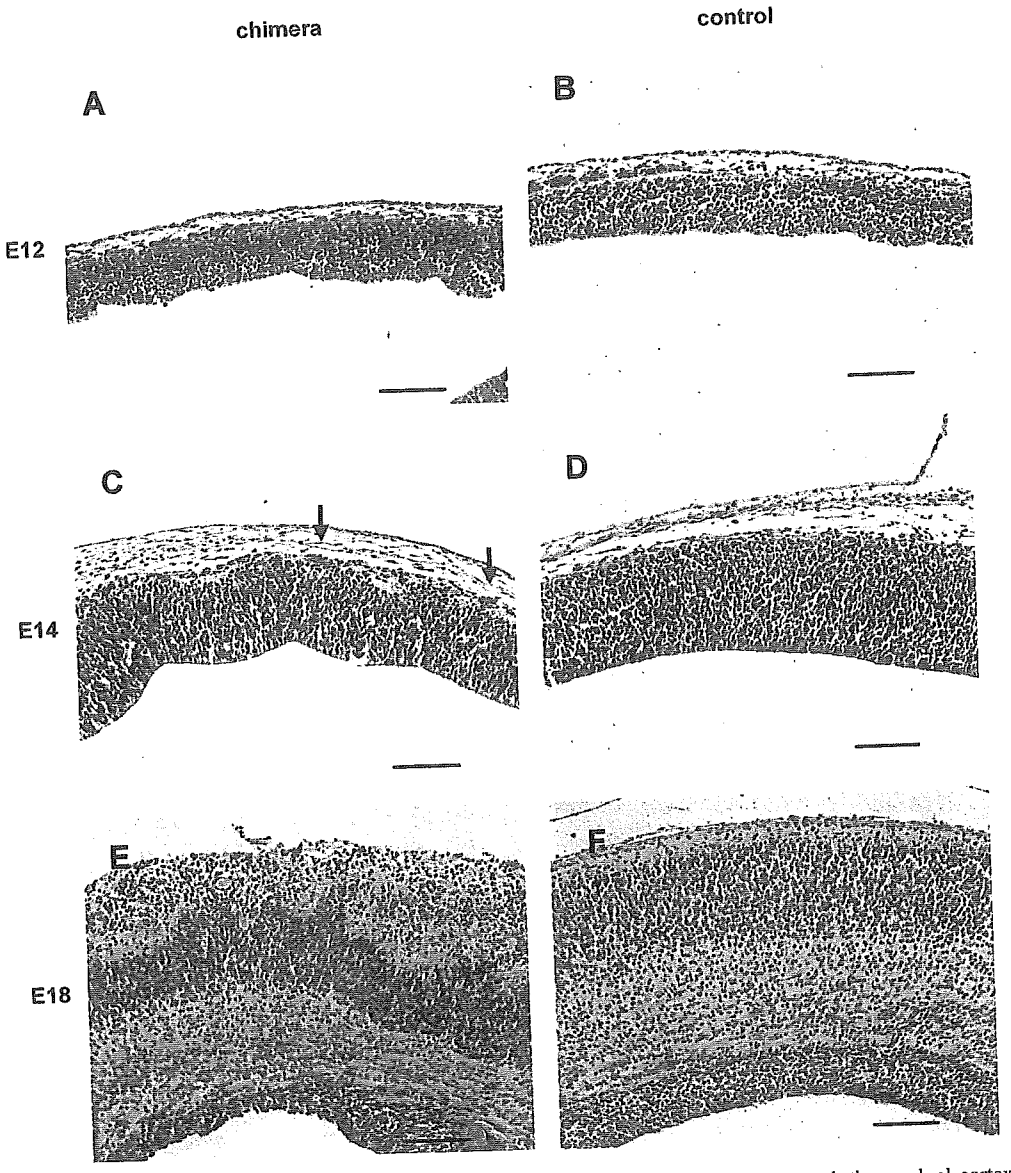

Fig. 1. Histological findings in the developing brain of fukutin-deficient chimeric mice. Sagittal sections through the cerebral cortex of fukutin-deficient chimeric (A, C, and E) and control (B, D, and F) embryos were analyzed by hematoxylin and eosin staining. (A and B) Sections of E12 embryos. There were no apparent differences between chimera and control. (C and D) Sections of E14 embryos. In chimeras, the cerebral cortex showed a wavy appearance, and ectopia could be observed as small groups of neurons invading into the subarachnoid space (arrows). (E and F) Sections of E18 embryos. In chimeras, the cortices were covered by abnormal neuroglial tissue, and laminar organization became distorted. Bars, 100 μm.

3.3. Neuronal migration

To determine whether fukutin deficiency affected neuronal migration itself, we labeled newly generated neurons with BrdU at E13 and analyzed the extent of their migration at E14 and E18. In both chimeras and controls, BrdU-labeled neurons were dispersed throughout entire cortex at E14 (Fig. 5A and B), indicating that the labeled neurons were migrating from the ventricular zone toward the pial surface. Quantitative analysis of radial distribution of BrdU-labeled neurons confirmed that the number and extent of the BrdU-labeled neurons did not differ between chimeras and controls at E14 (Fig. 5E), suggesting that cell proliferation in the ventricular zone and the initiation of neuronal migration toward the pial surface remain intact in chimeras. By E18, most BrdU-labeled neurons had localized to the cortical plate in controls (Fig. 5D). In E18 chimeras, most BrdU-labeled neurons also had localized to the cortical plate, although the cortical plate itself was undulating (Fig. 5C), consistent with our HE data (Fig. 1E). These observations suggest that neuronal migration itself is not affected in fukutin-deficient chimeras.

3.4. Radial glial fibers

During cortical development, neurons migrate along radial glial fibers. Each radial glial cell has its soma in the ventricular zone and elaborates its process that reaches

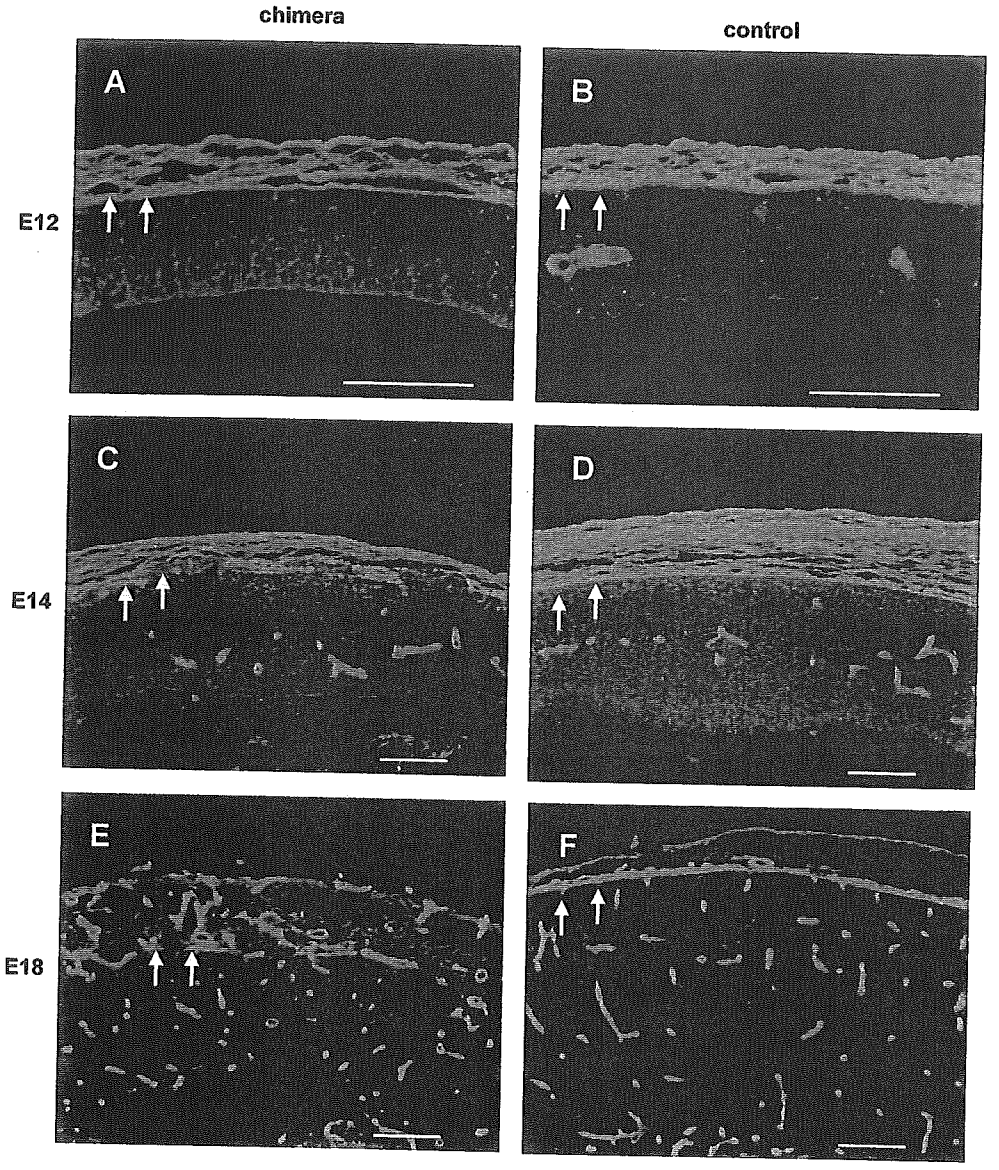

Fig. 2. Disruption of basal lamina caused by fukutin deficiency. Sagittal sections through the cerebral cortex of fukutin-deficient chimeric (A, C, and E) and control (B, D, and F) embryos were stained with an antibody against EHS laminin. In controls, the pial surface of the cortices was continuously covered with the BL, containing laminin, at all developmental stages (B, D, and F). In chimeras, the BL appeared intact only at E12 (A), and it became progressively disrupted in older embryos (C and E). Arrows indicate the position of the BL. Bars, 100 μm.

the pial surface, where it is anchored to the BL [16]. To determine whether the radial glial fibers had formed normally in fukutin-deficient chimeras, we analyzed their extension by immunohistochemistry, using antibodies against nestin. During the early stages of cortical development between E12 and E14, we observed no differences in alignment and density of the radial glial fibers between chimeras and controls (Fig. 6A–D). In E18 controls, the radial glial fibers in the cerebral cortex extended from the ventricular zone to the cortical surface, where they terminated consistently with their endfeet at the BL (Fig. 6F). In E18 chimeras, the radial glial fibers also extended from ventricular zone toward the cortical surface, but they terminated in variable locations (Fig. 6E). These abnormalities in glial fiber termination are thought to be secondary changes resulting from the disruption of the BL rather than a primary result of fukutin deficiency, because similar morphological changes have been reported to result from disruption of the BL [17].

4. Discussion

Neuronal migration plays an essential role in the formation of the mammalian brain during development [16]. Defects in neuronal migration lead to disorganization of cortical lamination and architecture, which cause mental retardation, epilepsy, and severe learning disabilities. The major pathological change in FCMD brain is polymicrogyria, and polymicrogyria in this disorder shows profound

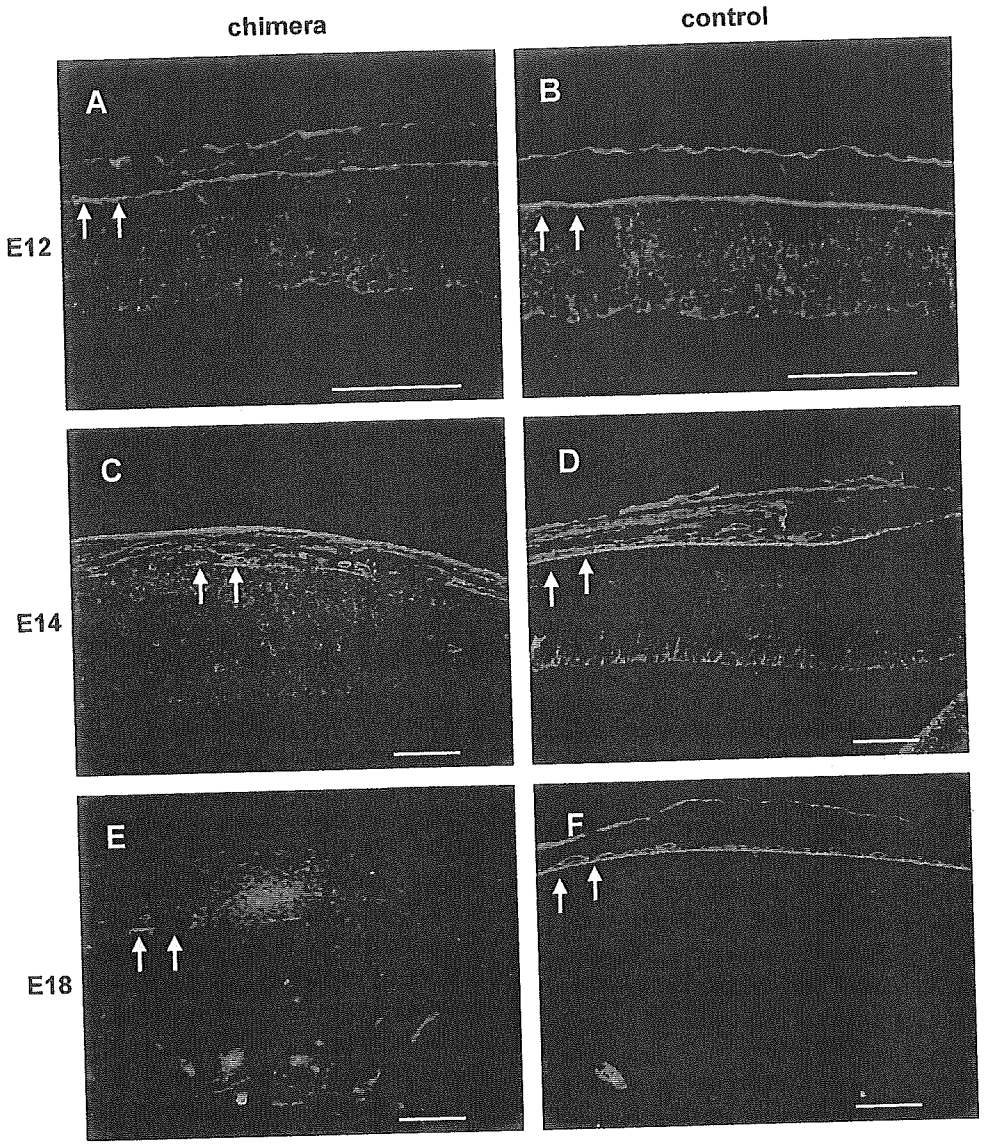

Fig. 3. Glycosylated α-dystroglycan in the developing brain of fukutin-deficient chimeric mice. Sagittal sections through the cerebral cortex of fukutin-deficient chimeric (A, C, and E) and control (B, D, and F) embryos were immunostained with IIH6C4. In chimeras, the immunoreactivity of glycosylated α-DG was progressively disrupted in the pial surface and paralleled those of laminin in both chimeras and controls. Arrows indicate the position of the BL. Bars, 100 μm.

disorganization of cortical lamination [1]. Pathological studies of brain tissue from FCMD fetuses and adults indicated that protrusion of neurons into the subarachnoid space through breaches in the GL–BL complex is a cardinal pathogenic process leading to the cortical dysplasia in this condition [8–10]. However, it remains unclear whether the primary defect caused by fukutin deficiency resides in the migrating neurons or in the GL–BL complex.

Studies of spatial and temporal fukutin expression in the brain have produced varied results [11–13], and the precise pattern of fukutin expression in the brain remains unclear. We previously demonstrated that *fukutin* mRNA is expressed specifically in neurons, including precursor neurons in the ventricular layer, neurons migrating through the intermediate layer, cortical neurons and Cajal–Retzius cells, but not in glial cells within the prenatal developing human cerebrum [11]. This neuronal expression suggests that fukutin may function in neuronal migration itself rather than GL and BL integrity. Another report also showed predominant expression of fukutin in neurons of the normal developing brain by immunohistochemistry, but the immunoreactivity of fukutin was markedly reduced in brain from FCMD patients [12]. In the fetal cerebrum, fukutin immunoreactivity was observed in Cajal–Retzius cells and the subpial granular layer [12]. This spatial and temporal pattern of fukutin expression indicates that fukutin may play a role in the termination of neuronal migration.

On the other hand, Yamamoto et al. [13] demonstrated that fukutin is expressed in glial cells, including astrocytes, which form the GL at the pial surface by their endfeet, suggesting an important role of GL for the genesis of FCMD brain. Electron microscopic examination revealed that BL

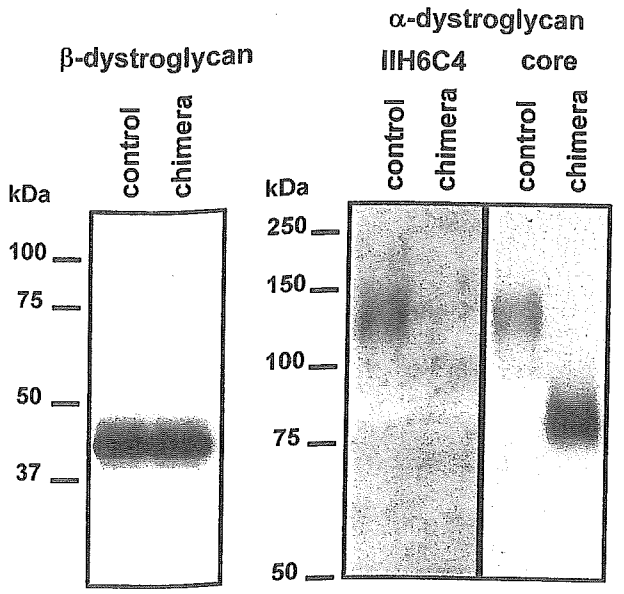

Fig. 4. Glycosylation defect of α-dystroglycan in the brain of fukutin-deficient chimeric mice. Western blot analyses of dystroglycan expression in WGA-enriched homogenates of E18 brain. β-DG is normally expressed, but glycosylated α-DG reactive to IIH6C4 is absent in the brain of chimeras. Core α-DG antibody shows that α-DG is expressed in the brain of chimera but reveals a decrease in molecular mass.

together with the GL has frequent breaches in FCMD fetus and adult brain [8–10]. Breaches of BL were also reported in skeletal muscle fibers in FCMD patients [18]. These observations support the hypothesis that BL fragility plays a key role in the pathophysiology of this disorder. Moreover, recent investigations revealed that mutations in genes encoding several BL components (laminin α5 or γ1, perlecan) [17,19,20], their cellular receptors (dystroglycan, β1 or α6 integrin) [21–23], and a molecule involved in signaling between BL components and the cytoskeleton (focal adhesion kinase) each disrupt normal assembly and remodeling of the cortical BL and result in cortical dysplasia in mice [24]. Intriguingly, these cortical phenotypes often strongly resemble those found in some forms of congenital muscular dystrophy, such as FCMD, WWS, and MEB. These findings indicate that disruption of the BL plays an important role in the pathogenesis of cortical dysplasia in these disorders.

In the present study, we have investigated the developing forebrain of fukutin-deficient chimeric mice, a unique and useful mouse model for FCMD, to elucidate the underlying pathogenic mechanism of a cortical dysplasia in FCMD. The BL of the cortical surface became discontinuous at E14, coinciding with the earliest time point at which neuronal ectopia could be observed, and showed progressive disruption during forebrain development. On the other hand, initiation of migration is apparently not altered in chimeric embryos. These observations suggest that fukutin deficiency results in the disruption of the BL but does not affect neuronal migration itself. Thus, disruption of the BL rather than aberrant neuronal migration appears to play a leading role in the pathogenesis of cortical dysplasia in FCMD. However, the termination of migration has not been investigated in this study. Subtle migration defects, caused by an impaired response to a molecular stop signal, might be present in fukutin-deficient chimeras, since previous studies demonstrate fukutin expression in Cajal–Retzius cells [11,12], which are essential for radial neuronal migration and for cortical lamination [25]. Investigation of the effects of neuron-specific disruption of fukutin may elucidate more clearly its neuronal function. In the developing cerebellum, granule-cell neurons migrate from the external granular layer towards inside. In this condition, the cerebellar polymicrogyria in FCMD may have different pathomechanism from that of cerebral polymicrogyria. Investigation of the developing cerebellum in fukutin-deficient chimeras, to see the role of basal lamina and migrating neurons in the cerebellar polymicrogyria, may also provide some clue to elucidate the pathogenesis of FCMD brain.

Although the details of fukutin function have not been clarified, results of several investigations suggest a functional linkage between fukutin and glycosylation of α-DG [4–7,15]. Dystroglycan is a component of the dystrophin–glycoprotein complex (DGC) in skeletal muscle. DGC serves as a link between the extracellular matrix and the subsarcolemmal cytoskeleton and is thought to protect muscle cells from contraction-induced damage [26]. In agreement with this hypothesis, structural defects in the DGC can disrupt the linkage between the extracellular matrix and cytoskeleton, leading to various types of muscular dystrophy [27]. Furthermore, recent investigations have defined the disruption of α-DG glycosylation as a newly recognized pathogenic mechanism for certain forms of muscular dystrophies, including FCMD [28,29]. All these conditions are caused by mutation of genes encoding known or putative glycosyltransferases, and common to all is the hypoglycosylation of α-DG [30–35]. Hypoglycosylated α-DG shows a decreased ability to bind its extracellular matrix ligands, including laminin, giving rise to progressive muscle degeneration [7]. Moreover, among these conditions, FCMD, MEB, WWS and myodystrophy (*myd*) mouse also show brain abnormalities, and it has been demonstrated that α-DG–ligand interactions are critical for normal cortical genesis as well as muscle integrity. In *myd* mice, hypoglycosylated α-DG abolishes binding activity of the ligands in brain as well as muscle, leading to disruption of the BL [7]. These observations suggest that abnormal α-DG–ligand interactions underlie the pathogenesis of cortical dysplasia in *myd* mice. In addition, brain-specific disruption of the dystroglycan gene (*Dag1*) in mice results in disruption of the pial surface BL and defects in neuronal migration that resembles the cortical dysplasia seen in FCMD, MEB,

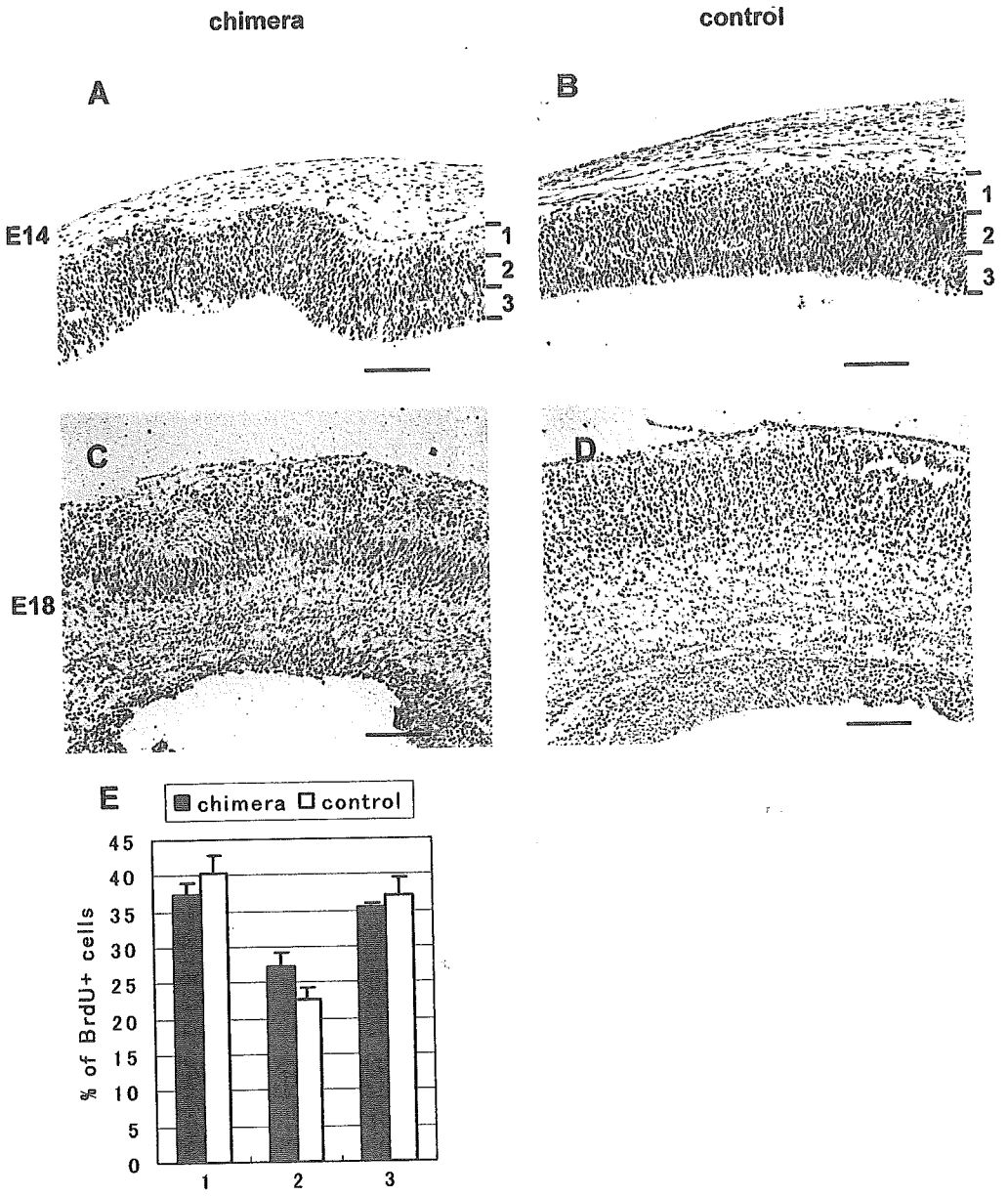

Fig. 5. Neuronal migration in the cortices of fukutin-deficient chimeric mice. Embryos labeled with BrdU at E13 were analyzed at E14 (A and B) and E18 (C and D). (A and B) At E14, the number and extent of labeled neurons (brown) did not differ between chimeras and controls. (C and D) In E18 control embryos, most BrdU-labeled neurons were localized in the cortical plate. Although the cortical plate was undulating in E18 chimeras, most BrdU-labeled neurons localized there. Bars, 100 μm. (E) Distribution of BrdU-labeled cells in E14 cortices, which are subdivided into three equidistant horizontal bands (A and B). Data are presented as percentages of labeled cells in a given horizontal band, referred to the total number of labeled cells throughout the cortical thickness. The difference between chimeras and controls is not significant. Error bars show standard errors of the means, $n=4$.

and WWS [21]. Therefore, loss of dystroglycan function, either through abnormal glycosylation or genetic deletion, results in disruption of the BL and abnormal neuronal migration. In addition to muscle and brain, recent report suggests that fukutin is involved in the glycosylation process of α-DG in various somatic organs, such as kidney, lung, gut and skin [36]. However, in FCMD patients, involvement of these somatic organs is not apparent in either morphogenesis or physiological function. Further investigation of the organ-specific differences in α-DG glycosylation may elucidate the molecular basis of selective involvement of muscle and brain in FCMD.

For the assembly of BL, dystroglycan is essential as a cell-surface receptor of laminin [37]. In murine dystroglycan–null embryos, loss of laminin assembly leads to disruption of Reichert's membrane, the first BL to form in the embryo, and causes early embryonic lethality [38]. *Fukutin*-null embryos, which also result in early embryonic lethality, demonstrate hypoglycosylation of α-DG and share a number of phenotypes with dystroglycan–null embryos,

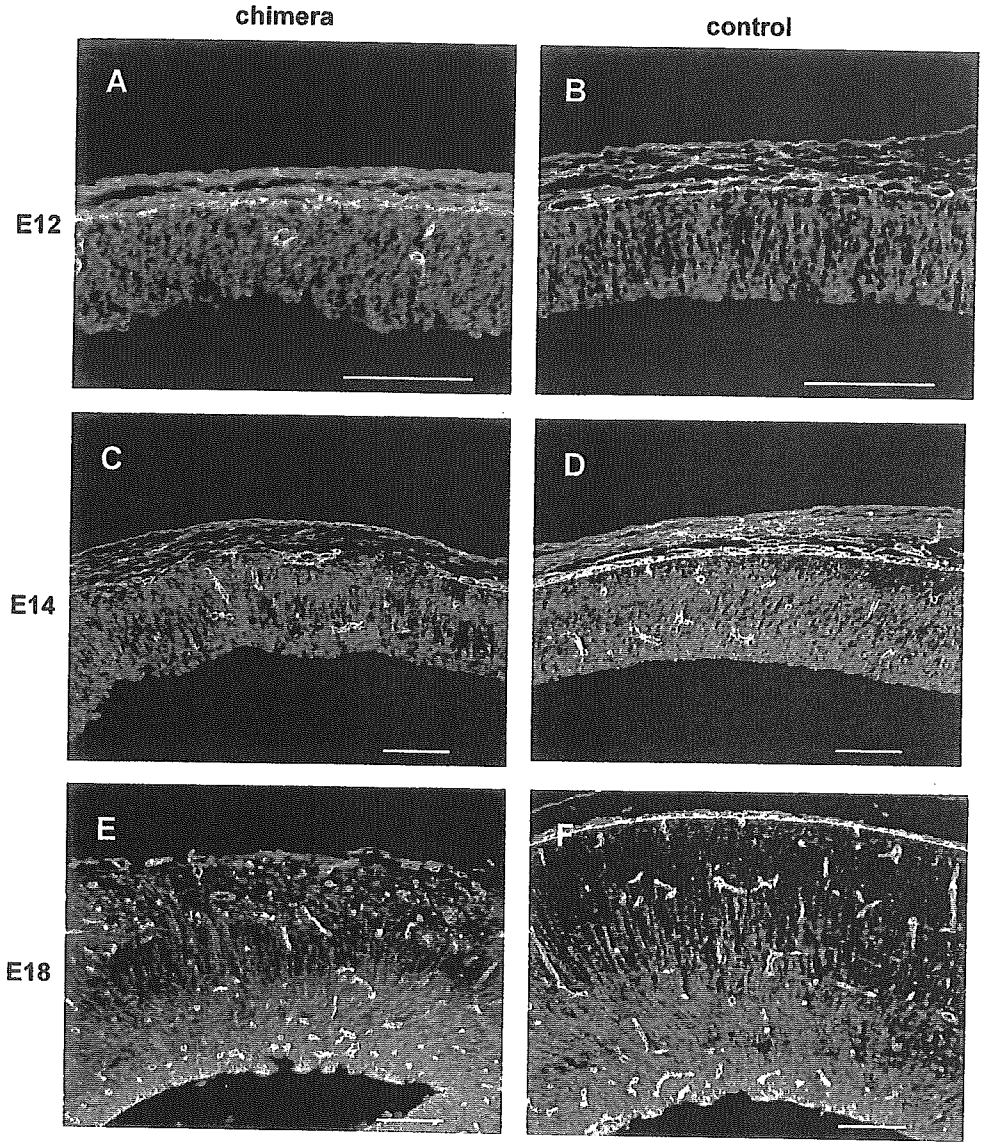

Fig. 6. Radial glial fibers in the developing cortices of fukutin-deficient chimeric mice. Sagittal sections through the cerebral cortex of fukutin-deficient chimeric (A, C, and E) and control (B, D, and F) embryos were double-immunostained for nestin (red) and laminin (green). There were no apparent differences in alignment and density of radial glial fibers (red) between chimeras and controls at E12 (A and B) and E14 (C and D). In E18 controls, radial glial fibers extended from the ventricular zone to the cortical surface, where they terminated consistently with their endfeet at the BL (yellow, immunofluorescent overlap) (F). In E18 chimeras, they terminated at variable locations (E). Bars, 100 μm.

suggesting that fukutin is also essential to BL integrity. However, in *fukutin*-null embryos, assembly of laminin was preserved, although subtle disorganization of BL is detectable under electron microscopy [14]. Thus *fukutin*-null embryos do not abolish the ability of BL formation completely. In this study, we demonstrated that the BL of cortical surface appeared intact only at early stage (E12) and it became progressively defective with age. These observations indicate that the BL is able to form but cannot be maintained in fukutin-deficient chimeras. In fukutin-deficient chimeras, residual fukutin protein might rescue the lethal BL dysfunction [14], but it is not sufficient to maintain BL integrity. We also demonstrated that progressive disruption of the BL in chimeras coincides strongly with a reduction in glycosylated α-DG. These observations point to a strong correlation between abnormal glycosylation of α-DG and disruption of the BL. Furthermore, laminin fails to bind α-DG from brains of fukutin-deficient chimeras [15]. These observations suggest that disruption of the BL, caused by the loss of interaction between hypoglycosylated α-DG and its ligands, plays a key role in the pathogenesis of cortical dysplasia in FCMD. Consistent with the brain abnormalities in fukutin-deficient chimeras, *myd* mice displays a variety of neuronal migration abnormalities [7,39]. Although there are some differences in neuronal phenotype between *myd* and fukutin-deficient

chimeric mice (for instance, fusion of cerebral hemispheric cortices is not observed in *myd* mouse, but is found in fukutin-deficient chimeras), the biochemical phenotype of brain tissue from fukutin-deficient chimeras is remarkably similar to that of *myd* brain [7]. Furthermore, *myd* mice also displays focal disruption of the BL, which results from the loss of α-DG–ligand interactions. Thus, BL fragility may be the common pathogenic mechanism underlying the cortical dysplasia seen in congenital muscular dystrophies with defective glycosylation of α-DG.

Acknowledgements

We thank Dr Kevin Campbell for providing anti-core α-DG antibody and Dr Jennifer Logan for editing the manuscript. This work was supported by a Health Science Research Grant, 'Research on Psychiatric and Neurological Diseases and Mental Health' and by a Research Grant for Nervous and Mental Disorders (14B-4), both from the Ministry of Health, Labor, and Welfare of Japan; and by the 21st Century COE program from the Ministry of Education, Culture, Sports, Science, and Technology of Japan.

References

[1] Fukuyama Y, Osawa M, Suzuki H. Congenital progressive muscular dystrophy of the Fukuyama type—clinical, genetic and pathological considerations. Brain Dev 1981;3:1–29.
[2] Santavuori P, Somer H, Sainio K, et al. Muscle–eye–brain disease (MEB). Brain Dev 1989;11:147–53.
[3] Dobyns WB, Pagon RA, Armstrong D, et al. Diagnostic criteria for Walker–Warburg syndrome. Am J Med Genet 1989;32:195–210.
[4] Kobayashi K, Nakahori Y, Miyake M, et al. An ancient retrotransposal insertion causes Fukuyama-type congenital muscular dystrophy. Nature 1998;394:388–94.
[5] Aravind L, Koonin EV. The fukutin protein family-predicted enzymes modifying cell-surface molecules. Curr Biol 1999;9:R836–R7.
[6] Hayashi YK, Ogawa M, Tagawa K, et al. Selective deficiency of α-dystroglycan in Fukuyama-type congenital muscular dystrophy. Neurology 2001;57:115–21.
[7] Michele DE, Barresi R, Kanagawa M, et al. Post-translational disruption of dystroglycan–ligand interactions in congenital muscular dystrophies. Nature 2002;418:417–21.
[8] Nakano I, Funahashi M, Takada K, Toda T. Are breaches in the glia limitans the primary cause of the micropolygyria in Fukuyama-type congenital muscular dysptophy (FCMD)? Pathological study of the cerebral cortex of an FCMD fetus Acta Neuropathol 1996;91:313–21.
[9] Yamamoto T, Toyoda C, Kobayashi M, Kondo E, Saito K, Osawa M. Pial–glial barrier abnormalities in fetuses with Fukuyama congenital muscular dystrophy. Brain Dev 1997;19:35–42.
[10] Saito Y, Murayama S, Kawai M, Nakano I. Breached cerebral glia limitans–basal lamina complex in Fukuyama-type congenital muscular dystrophy. Acta Neuropathol 1999;98:330–6.
[11] Sasaki J, Ishikawa K, Kobayashi K, et al. Neuronal expression of the fukutin gene. Hum Mol Genet 2000;9:3083–90.
[12] Saito Y, Mizuguchi M, Oka A, Takashima S. Fukutin protein is expressed in neurons of the normal developing human brain but is reduced in Fukuyama-type congenital muscular dystrophy brain. Ann Neurol 2000;47:756–64.
[13] Yamamoto T, Kato Y, Karita M, et al. Fukutin expression in glial cells and neurons: implication in the brain lesions of Fukuyama type congenital muscular dystrophy. Acta Neuropathol 2002;104: 217–24.
[14] Kurahashi H, Taniguchi M, Meno C, et al. Basement membrane fragility underlies embryonic lethality in *fukutin*–null mice. Neurobiol Dis 2005;19:208–17.
[15] Takeda S, Kondo M, Sasaki J, et al. Fukutin is required for maintenance of muscle integrity, cortical histiogenesis and normal eye development. Hum Mol Genet 2003;12:1449–59.
[16] Marin O, Rubenstein JL. Cell migration in the forebrain. Annu Rev Neurosci 2003;26:441–83.
[17] Halfter W, Dong S, Yip YP, Willem M, Mayer U. A critical function of the pial basement membrane in cortical histogenesis. J Neurosci 2002;22:6029–40.
[18] Ishii H, Hayashi YK, Nonaka I, Arahata K. Electron microscopic examination of basal lamina in Fukuyama congenital muscular dystrophy. Neuromusc Disord 1997;7:191–7.
[19] Miner JH, Cunningham J, Sanes JR. Roles for laminin in embryogenesis: exencephaly, syndactyly, and placentopathy in mice lacking the laminin α5 chain. J Cell Biol 1998;143:1713–23.
[20] Costell M, Gustafsson E, Aszodi A, et al. Perlecan maintains the integrity of cartilage and some basement membranes. J Cell Biol 1999;147:1109–22.
[21] Moore SA, Saito F, Chen J, et al. Deletion of brain dystroglycan recapitulates aspects of congenital muscular dystrophy. Nature 2002; 418:422–5.
[22] Graus-Porta D, Blaess S, Senften M, et al. β1-Class integrins regulate the development of laminae and folia in the cerebral and cerebellar cortex. Neuron 2001;31:367–79.
[23] Georges-Labouesse E, Mark M, Messaddeq N, Gansmuller A. Essential role of α6 integrins in cortical and retinal lamination. Curr Biol 1998;8:983–6.
[24] Beggs HE, Schahin-Reed D, Zang K, et al. FAK deficiency in cells contributing to the basal lamina results in cortical abnormalities resembling congenital muscular dystrophies. Neuron 2003;40: 501–14.
[25] Sarnat HB, Flores-Sarnat L. Cajal–Retzius and subplate neurons: their role in cortical development. Eur J Paediatr Neurol 2002;6:91–7.
[26] Durbeej M, Campbell KP. Muscular dystrophies involving the dystrophin–glycoprotein complex: an overview of current mouse models. Curr Opin Genet Dev 2002;12:349–61.
[27] Campbell KP. Three muscular dystrophies: loss of cytoskeleton–extracellular matrix linkage. Cell 1995;80:675–9.
[28] Muntoni F, Brockington M, Blake DJ, Torelli S, Brown SC. Defective glycosylation in muscular dystrophy. Lancet 2002;360:1419–21.
[29] Grewal PK, Hewitt JE. Glycosylation defects: a new mechanism for muscular dystrophy? Hum Mol Genet 2003;12:R259–R64.
[30] Yoshida A, Kobayashi K, Manya H, et al. Muscular dystrophy and neuronal migration disorder caused by mutations in a glycosyltransferase, POMGnT1. Dev Cell 2001;1:717–24.
[31] Grewal PK, Holzfeind PJ, Bittner RE, Hewitt JE. Mutant glycosyltransferase and altered glycosylation of α-dystroglycan in the myodystrophy mouse. Nat Genet 2001;28:151–4.
[32] Brockington M, Blake DJ, Prandini P, et al. Mutations in the fukutin-related protein gene (FKRP) cause a form of congenital muscular dystrophy with secondary laminin α2 deficiency and abnormal glycosylation of α-dystroglycan. Am J Hum Genet 2001;69: 1198–209.
[33] Brockington M, Yuva Y, Prandini P, et al. Mutations in the fukutin-related protein gene (*FKRP*) identify limb girdle muscular dystrophy 2I as a milder allelic variant of congenital muscular dystrophy MDC1C. Hum Mol Genet 2001;10:2851–9.
[34] Beltran-Valero de Bernabe D, Currier S, Steinbrecher A, et al. Mutations in the *O*-mannosyltransferase gene POMT1 give rise to the severe neuronal migration disorder Walker–Warburg syndrome. Am J Hum Genet 2002;71:1033–43.

[35] Longman C, Brockington M, Torelli S, et al. Mutations in the human LARGE gene cause MDC1D, a novel form of congenital muscular dystrophy with severe mental retardation and abnormal glycosylation of α-dystroglycan. Hum Mol Genet 2003;12: 2853–61.

[36] Saito Y, Yamamoto T, Ohtsuka-Tsurumi E, et al. Fukutin expression in mouse non-muscle somatic organs: its relationship to the hypoglycosylation of α-dystroglycan in Fukuyama-type congenital muscular dystrophy. Brain Dev 2004;26: 469–79.

[37] Henry MD, Campbell KP. A role for dystroglycan in basement membrane assembly. Cell 1998;95:859–70.

[38] Williamson RA, Henry MD, Daniels KJ, et al. Dystroglycan is essential for early embryonic development: disruption of Reichert's membrane in *Dag1*-null mice. Hum Mol Genet 1997;6:831–41.

[39] Holzfeind PJ, Grewal PK, Reitsamer HA, et al. Skeletal, cardiac and tongue muscle pathology, defective retinal transmission, and neuronal migration defects in the Large^{myd} mouse defines a natural model for glycosylation-deficient muscle–eye–brain disorders. Hum Mol Genet 2002;11:2673–87.

Available online at www.sciencedirect.com
SCIENCE DIRECT®
Biochemical and Biophysical Research Communications 333 (2005) 131–137
BBRC
www.elsevier.com/locate/ybbrc

β4GalT-II is a key regulator of glycosylation of the proteins involved in neuronal development

Norihiko Sasaki [a,e], Hiroshi Manya [b], Reiko Okubo [a], Kazuhiro Kobayashi [c], Hideki Ishida [d,e], Tatsushi Toda [c], Tamao Endo [b], Shoko Nishihara [a,e,*]

[a] *Laboratory of Cell Biology, Department of Bioinformatics, Faculty of Engineering, Soka University 1-236 Tangi-cho, Hachioji, Tokyo 192-8577, Japan*
[b] *Glycobiology Research Group, Tokyo Metropolitan Institute of Gerontology, Foundation for Research on Aging and Promotion of Human Welfare, 35-2 Sakae-cho, Itabashi-ku, Tokyo 173-0015, Japan*
[c] *Division of Clinical Genetics, Department of Medical Genetics, Osaka University Graduate School of Medicine, 2-2-B9 Yamadaoka, Suita, Osaka 565-0871, Japan*
[d] *The Noguchi Institute, 1-8-1 Kaga, Itabashi-ku, Tokyo 173-0003, Japan*
[e] *Core Research for Evolutional Science and Technology (CREST) of Japan Science and Technology Agency (JST), Kawaguchi Center Building, 4-1-8 Hon-cho, Kawaguchi, Saitama 332-0012, Japan*

Received 29 April 2005
Available online 31 May 2005

Abstract

Seven members of the human β1,4-galactosyltransferase (β4GalTs) have been identified and characterized by many groups. β4GalTs play important roles in the extension of N- and O-linked glycans involved in several biological events. However, it has not been clear which β4GalTs can act on glycoproteins, such as α-dystroglycan and Notch receptors, involved in neuronal development. To clarify which β4GalTs can function, we determined the enzyme activities toward such motifs and the transcript levels in human normal tissues. Among human β4GalTs, both β4GalT-I and β4GalT-II could act efficiently on all substrates, but the relative activity of β4GalT-II was higher than that of β4GalT-I. Transcript of *β4GalT-I* was widely expressed except for brain, and on the other hand, that of *β4GalT-II* was expressed at high levels in the brain. Thus, these results suggest that among human β4GalTs, β4GalT-II is a major regulator of the synthesis of glycans involved in neuronal development.

Keywords: β4GalT-II; α-Dystroglycan; Notch receptors

The Galβ1-4GlcNAc structure has been found in N-linked and O-linked glycans of several glycoproteins, which play important roles in many biological events. Among those glycoproteins, α-dystroglycan (α-DG) and Notch receptors are biologically important in the development of the nervous system. DG is a highly glycosylated component of the dystrophin–glycoprotein complex in muscle and brain [1,2]. α-DG is extracellular subunit of DG and includes *O*-mannosyl oligosaccharides, which are required for binding to laminin, neurexin, and agrin [3–6]. Recently, several congenital muscular dystrophies (CMDs) exhibiting neuronal migration disorders have been reported as defective in the enzymes required for the synthesis of *O*-mannosyl oligosaccharides [6–8]. Notch receptors are glycoproteins, which are modified in epidermal growth factor-like domains by O-linked oligosaccharides [9,10], and play important roles in a wide range of developmental processes. It has been demonstrated that the glycosylation on Notch receptors is essential for normal Notch signaling [11,12], and modulation of glycosylation by

* Corresponding author. Fax: +81 426 91 9315.
E-mail address: shoko@t.soka.ac.jp (S. Nishihara).

0006-291X/$ - see front matter © 2005 Elsevier Inc. All rights reserved.
doi:10.1016/j.bbrc.2005.05.082

O-fucosyltransferase 1 (OFUT1) and Fringe changes Notch–ligand interactions [13].

Previously, seven members of the human β1,4-galactosyltransferase (β4GalTs) have been identified and characterized [14–22] in terms of substrate specificity as the following. β4GalT-I is the first isolated galactosyltransferase and acts on non-reducing terminal GlcNAc as an acceptor [14,15]. In the presence of α-lactalbumin, the enzyme can function as lactose synthase [23]. β4GalT-I has been demonstrated to play important roles in poly-*N*-acetyllactosamine extension [24]. β4GalT-II and β4GalT-III act on GlcNAc residues in several glycoproteins and glycolipids, but only β4GalT-II can function as lactose synthase like β4GalT-I, and β4GalT-III efficiently catalyzes the synthesis of the first *N*-acetyllactosamine unit in lactoseries glycolipids [16]. β4GalT-IV acts on neolactoseries glycolipids [17], poly-*N*-acetyllactosamine in core 2 [25], and GlcNAc 6-*O*-sulfate [26]. β4GalT-V has been suggested to be involved in the *O*-glycosylation of core 2 and core 6 [27], and also to participate in the galactosylation of the GlcNAcβ1-6 branch, which is synthesized by GlcNAcT-V [28]. β4GalT-VI has been shown to have lactosylceramide synthase activity [19,20]. β4GalT-VII is galactosyltransferase-I, which is involved in the first galactosylation of the proteoglycan linkage region [21,22]. Although the substrate specificities of these seven β4GalTs have been extensively studied as above, it remained unclear which enzymes can act on a disaccharide (GlcNAcβ1-2Man) on α-DG and a disaccharide (GlcNAcβ1-3Fuc) on Notch receptors.

In the present study, we examined which human β4GalTs act on each of the above substrates and determined their transcript levels in normal tissues. Then, we discussed the possibility that β4GalT-II is a candidate for a key enzyme in neuronal development.

Materials and methods

Construction of human β4GalTs expression vector and purification of FLAG-tagged recombinant human β4GalTs enzyme. The putative catalytic domain of human β4GalTs enzyme (β4GalT-I, 52–398a.a.; β4GalT-II, 42–372a.a.; β4GalT-III, 31–393a.a.; β4GalT-IV, 55–344a.a.; β4GalT-V, 46–388a.a.; β4GalT-VI, 37–382a.a.; β4GalT-VII, 60–327a.a.) was expressed as a secreted protein fused with a FLAG tag in *Sf21* cells according to the instruction manual of GATEWAY Cloning Technology (Invitrogen). A ~1.3 kb DNA fragment was amplified by two-step PCR. The first PCR used the Bluescript containing each human *β4GalTs* DNA as a template, and the following primers: *T-I*, forward 5′-AAAAAGCAGGCTCCCAACTGGTCG GAGTCT-3′ and reverse 5′-AGAAAGCTGGGTCAAAACGCTA GCTCGGTG-3′; *T-II*, forward 5′-AAAAAGCAGGCTTCTTCAGC CGCTTCAGTG-3′ and reverse 5′-AGAAAGCTGGGTCCGAGA GCCTCTGTCCAT-3′; *T-III*, forward 5′-AAAAAGCAGGCTGCT TCCGAAGTCTCAGTG-3′ and reverse 5′-AGAAAGCTGGGTCC CCATGAATTCGGTTTC-3′; *T-IV*, forward 5′-AAAAAGCAGGC TCCCTCATTTTGGGGAAGG-3′ and reverse 5′-AGAAAGCTG GGTCAGGGTCATGCACCAAAC-3′; *T-V*, forward 5′-AAAAAG CAGGCTTGATGCAAGCCCAAGGCA-3′ and reverse 5′-AGA AAGCTGGGTCGGTGGGTAAAGCAAACG-3′; *T-VI*, forward 5′-AAAAAGCAGGCTCAGGCATCGCCAACACAT-3′ and reverse 5′-AGAAAGCTGGGTTCTACCTTGCCACGACAG-3′; *T-VII*, forward 5′-AAAAAGCAGGCTCTGAGCACTGGGAAGAAG-3′ and reverse 5′-AGAAAGCTGGGTCACTGTCCATCCAGCTCA-3′. The second PCR used the first PCR product as a template, the forward primer 5′-GGGGACAAGTTTGTACAAAAAAGCAGGCT-3′, and the reverse primer 5′-GGGGACAAGTTTGTACAAAAAAGC AGGCT-3′. The forward and reverse primers were flanked with *att*B1 and *att*B2 sequences, respectively, to create the recombination sites. The amplified fragment was recombined between the *att*P1 and *att*P2 sites of the pDONR 201 vector using the BP CLONASE Enzyme Mix (Invitrogen). Then, the insert was transferred between the *att*R1 and *att*R2 sites of pVL1393-FLAG to yield pVL1393-FLAG vector. PVL1393-FLAG is an expression vector derived from pVL1393 (Pharmingen, San Diego, CA) and contains a fragment encoding the signal peptide of human immunoglobulin κ (MHFQVQIFSFLLISASVIMSRG), the FLAG tag (DYKDDDDK), and a conversion site for the GATEWAY system.

PVL1393-FLAG-*β4GalTs* were cotransfected with BaculoGold viral DNA (Pharmingen, San Diego, CA) into *Sf21* insect cells according to the manufacturer's instructions and incubated for 3 days at 27 °C to produce recombinant viruses. *Sf21* cells were infected with recombinant viruses at a multiplicity of infection of five and incubated for 72 h at 27 °C. The culture supernatants were harvested and mixed with 100 μl anti-FLAG M1 AFFINITY GEL (Sigma). The protein–gel mixture was washed twice with 50 mM Tris-buffered saline (50 mM Tris–HCl, pH 7.4, and 150 mM NaCl) containing 1 mM $CaCl_2$ and eluted with 100 μl of 100 μg/ml FLAG peptide in 10 mM Tris-buffered saline (Sigma). GalT assay was determined as described below.

Western blot analysis. The enzymes purified above were subjected to 12.5% SDS–polyacrylamide gel electrophoresis, followed by Western blot analysis. The separated proteins were transferred to a Hybond-P membrane (Amersham Bioscience). The membrane was probed with anti-FLAG M2-peroxidase conjugate (Sigma) and stained with Konica Immunostaining HRP-1000 (Konica, Tokyo, Japan). The intensity of positive bands on Western blotting was measured by a densitometer to determine the amount of the purified enzyme using FLAG-BAP Control Protein (Sigma).

Assay of GalT activity toward fluorescein labeled substrate. To determine the enzyme activity, UDP-Gal (Sigma) was utilized as a donor substrate and for various acceptor substrates. The synthesis of GlcNAcβ1-3Fuc-dansyl (DNS) is described below. Glycosylation of 2-(trimethylsilyl)ethyl 2,4-di-*O*-benzyl-β-L-fucopyranoside with phenyl 3,4,6-tri-*O*-acetyl-2-deoxy-2-phthalimido-1-thio-β-D-glucopyranoside using *N*-iodosuccinimide-trifluoromethanesulfonic acid as a promoter gave the disaccharide derivative in 78% yield. The disaccharide derivative was converted into phenyl thioglycoside, via removal of the phthaloyl group, N-acetylation, cleavage of 2-(trimethylsilyl)ethyl group, O-acetylation, and reaction with thiophenol in the presence of $BF_3 \cdot OEt_2$. Glycosylation of 2-(benzyloxycarbonylamino)ethanol with the phenyl thioglycoside of the disaccharide using dimethyl(methylthio)sulfonium triflate as a promoter gave the α-glycoside (72%), which was transformed, via de-O-acetylation, reductive removal of benzyl groups and benzyloxycarbonyl group, and coupling of 6-(dansylamino)hexanoic acid succinimidyl ester into the desired substrate GlcNAcβ1-3Fuc-DNS.

GlcNAcβ1-2Man was obtained from Honen (Tokyo, Japan). GlcNAcβ1-3(Galβ1-4GlcNAcβ1-3)$_2$-2AB(2-aminobenzamide) [29] and GlcNAcβ1-2Man-2AB were prepared by labeling the corresponding oligosaccharides with 2AB according to the instruction manual of the Signal 2AB glycan labeling kit (Oxford GlycoScience, UK).

For the reaction in the GalT assay, 14 mM Hepes (pH 7.4) containing 0.1% Triton X-100, 0.25 mM UDP-Gal, 11 mM $MnCl_2$, and 0.6 mM acceptor substrate was used. A 5 μl volume of enzyme solution